Environmental Science and Pollution Research
https://doi.org/10.1007/s11356-023-28162-z

RESEARCH ARTICLE

# Phytoremediation potential modulated by structural and functional traits in a saline desert halophyte *Fagonia indica* Burm. f

**Nargis Naz[1] · Sana Fatima[2] · Mansoor Hameed[3] · Muhammad Sajid Aqeel Ahmad[3] · Syed Mohsan Raza Shah[4] · Farooq Ahmad[3] · Majid Anwar[5] · Sana Basharat[3] · Ansa Asghar[3] · Muhammad Ashraf[6]**

Received: 30 September 2022 / Accepted: 3 June 2023


## Abstract

Using halophytes for phytoremediation is an environmentally friendly technique, now gaining importance all over the world. *Fagonia indica* Burm. f. (Indian Fagonia) is primarily distributed in salt-affected lands of the Cholistan Desert and surrounding habitats. Four populations with three replications from salt-affected habitats were collected from natural habitats to evaluate structural and functional adaptation for salinity tolerance and phytoremediation of hypersaline habitats. The populations collected from the highest saline sites Pati Sir (PS) and Ladam Sir (LS) had restricted growth habit, increased accumulation of $K^+$ and $Ca^{2+}$ along $Na^+$ and $Cl^-$, more excretion of $Na^+$ and $Cl^-$, increased cross-sectional area of root and stem, larger exodermal and endodermal cells in roots, and broad metaxylem area. Sclerification in stem was high in population. Specific modifications in leaves were reduced stomatal area and increased adaxial epidermal cell area. Important traits associated with phytoremediation potential of *F. indica* populations (Pati Sir and Ladam Sir) were deeper roots and taller plants, increased density of salt glands on leaf surface, and high excretion of $Na^+$. Additionally, higher bio-concentration factor, translocation factor, and dilution factor for Na and $Cl^-$ in same Ladam Sir and Pati Sir population were identified as key phytoremediation attributes. The plants of *F. indica* colonizing high salinities (Pati Sir and Ladam Sir) were, therefore, more efficient in phytoremediation of saline soils as these populations accumulated and/or excrete toxic salts. Density of salt glands remarkably increased in the Pati Sir population collected from the highest salinity. This population accumulated and excreted the highest amount of $Na^+$ and $Cl^-$. The dilution factor of $Na^+$ and $Cl^-$ ions was also the highest in this population. Anatomical modifications such as root and stem cross-sectional areas, proportion of storage parenchyma, and broad metaxylem vessels were the maximum in Pati Sir population. These modifications indicate not only better salt tolerance of the Pati Sir population but also better in accumulation and excretion of toxic salts. This population can potentially rehabilitate hypersaline uncultivated lands through green reclamation.

**Keywords** Eco-morphological · Hypersaline · Leaf succulence · Salinity tolerance · Sclerification · Saline habitats

## Abbreviations

**Site**

| | |
|---|---|
| DF | Derawar Fort |
| TWT | Traway Wala Toba |

Responsible Editor: Elena Maestri

✉ Mansoor Hameed
hameedmansoor@yahoo.com

[1] Department of Botany, The Islamia University of Bahawalpur, Bahawalpur 63100, Pakistan

[2] Department of Botany, The Government Sadiq Collage Women University, Bahawalpur 63100, Pakistan

[3] Department of Botany, University of Agriculture Faisalabad, Faisalabad 38000, Pakistan

[4] Division of Science and Technology, Department of Botany, University of Education, Lahore 54000, Pakistan

[5] Department of Pharmacology, Riphah International University, Lahore 54000, Pakistan

[6] Institute of Molecular Biology and Biotechnology, The University of Lahore, Lahore 54000, Pakistan

Published online: 10 June 2023

| | |
|---|---|
| LS | Ladam Sir |
| PS | Pati Sir |

**Soil attributes**

| | |
|---|---|
| OSP | Saturation percentage |
| OMC | Moisture content |
| OOM | Organic matter |
| OAR | Average rainfall |
| OTP | Temperature |
| OPH | PH |
| OEC | ECe |
| ONA | $Na^+$ |
| OK | $K^+$ |
| OCA | $Ca^{2+}$ |
| OMG | $Mg^{2+}$ |
| OCL | $Cl^-$ |
| ONO | $NO_3^-$ |
| OPO | $PO_4^{3-}$ |

**Ecological characteristics**

| | |
|---|---|
| ERF | Relative frequency |
| ERD | Relative density |
| EIV | Importance value |
| ERC | Relative cover |

**Morphological characteristics**

| | |
|---|---|
| MLA | Leaf area |
| MRL | Root length |
| MSL | Shoot length |

**Ionic contents**

| | |
|---|---|
| ISN | Shoot $Na^+$ |
| IRN | Root $Na^+$ |

**ISK-Shoot $K^+$**

| | |
|---|---|
| IRK | Root $K^+$ |
| ISC | Shoot $Ca^{2+}$ |
| IRC | Root $Ca^{2+}$ |
| ISL | Shoot $Cl^-$ |
| IRL | Root $Cl^-$ |
| ISM | Shoot $Mg^{2+}$ |
| IRM | Root $Mg^{2+}$ |
| ISP | Shoot $PO_4^{3-}$ |
| IRP | Root $PO_4^{3-}$ |
| ISO | Shoot $NO_3^-$ |
| IRO | Root $NO_3^-$ |

**Excreted ions**

| | |
|---|---|
| XNA | Excreted $Na^+$ |
| XK | Excreted $K^+$ |
| XCL | Excreted $Cl^-$ |
| XPO | Excreted $PO_4^{3-}$ |
| XNO | Excreted $NO_3^-$ |
| XMG | Excreted $Mg^{2+}$ |
| XCA | Excreted $Ca^{2+}$ |

**Root anatomical parameters**

| | |
|---|---|
| RRA | Root area |
| RXA | Exodermis cell area |
| RHA | Hypodermis cell area |
| RCT | Cortex thickness |
| RCA | Cortex cell area |
| REA | Endodermis cell area |
| RPA | Pericycle cell area |
| RMA | Metaxylem area |
| RVA | Phloem area |

**Stem anatomical parameters**

| | |
|---|---|
| SSA | Stem area |
| SEA | Epidermis cell area |
| SHA | Hypodermis cell area |
| SCT | Cortex thickness |
| SCA | Cortex cell area |
| SMA | Metaxylem area |
| SVA | Phloem area |
| SPT SPA | Pith cell area |
| SSB | Sclerenchyma bundle area |
| SPC | Palisade cell area |
| SSC | Spongy cell area |

**Leaf anatomical parameters**

| | |
|---|---|
| LSN | Lower epidermal stomata number |
| LUS | Upper epidermal stomata number |
| LSA | Lower epidermal stomata area |
| LUA | Upper epidermal stomata area |
| LMT | Midrib thickness |
| LLT | Lamina thickness |
| LEC | Lower epidermis cell area |
| LUC | Upper epidermis cell area |
| LCT | Upper epidermis cell area |
| LCA | Cortical cell area |
| LPA | Palisade cell area |
| LSC | Spongy cell area |
| LMA | Metaxylem area |
| LVA | Phloem area |

## Introduction

Cholistan is the hottest saline desert in Pakistan located in southern Punjab, which spreads over an area of 26,000 $km^2$. Ecologically, this sandy desert is divided into distinct zones such as sand dunes, hypersaline flats, and occasional dried surface clay pans (Ahmad and Eram 2011). A considerable variation in environmental conditions exists throughout the Cholistan Desert and exposed to multiple stresses like salinity, drought, and heat. These environmental constraints enforce a serious threat to plant species. The colonizing species acquire several structural and functional adaptive components to thrive in such environmental adversaries. The

Cholistan possesses a specific floristic composition, where dominant grasses are *Stipagrostis plumosa* (L.) Munro ex T. Anderson, *Cenchrus ciliaris* L., *Cenchrus biflorus* Roxb., *Lasiurus scindicus* Henrard, *Aristida adscensionis* L., *Panicum turgidum* Forssk., *Ochthochloa compressa* (Forssk.) Hilu, *Aeluropus lagopoides* (L.) Thwaites, *Sporobolus ioclados* (Trin.) Nees, and *Cymbopogon jwarancusa* (Jones) Schult. (Ahmed et al. 2014).

Soil salinization mainly occurs due to an excessive number of soluble salts in the soil. It is a key factor causing desertification and is associated with soil erosion, degradation, and loss of arable lands (Castro and Santos 2020). Desert plants exhibit several eco-morphological, physiological, and anatomical adaptations in response to salinity. Morphological adaptations in desert plants include thickened and smaller leaves, succulence, extensive deposition of wax, and increased trichome density (Mansoor et al. 2019). Anatomical modifications in desert plants include thick cuticle and epidermis, sclerification in soft tissues, smaller and fewer stomata, higher proportion of storage tissues, and thickened endodermis (Naz et al. 2016).

In addition to traditional methods involving mechanical or chemical treatment of contaminated substrate, science has given us new opportunities to use microorganisms (bioremediation) and plants (phytoremediation) to transfer or remove toxic substances from the environment (Gavrilescu 2022). Restoration of saline lands has been attempted by several researcher by using fast-growing salt accumulators, i.e., green remediation. The examples are *Suaeda maritima* (L.) Dumort., *Sesuvium portulacastrum* (L.) L. (Ravindran et al. 2007), *Tamarix aphylla* (L.) Karst., *Atriplex nummularia* Lindl., *Atriplex halimus* L. (Al-Nasir 2009), *Halopeplis perfoliata* (Forssk.) Schweinf. & Asch., *Salicornia europaea* L., *Salsola soda* L., and *Tetraena qatarensis* (Hadidi) Beier & Thulin (Yasseen and Al-Thani 2022). Desalination by biological approach is based on three main processes: (a) release of $Na^+$ from cation exchange sites, (b) $Na^+$ leaching, and/or (c) phytodesalination through $Na^+$ uptake by roots and accumulation in shoots. Desalination through plants uses the cheapest way for phytoremediation of salt-affected soils, as salt accumulators can accumulate salts up to 50% of their dry weights (Khan and Weber 2006). Accumulation of these $Na^+$ and $Cl^-$ is relatively higher in the vacuoles of mesophyll parenchyma and bundle sheath cells. The cytosolic concentration of $Na^+$ retains up to 30 mM in glycophytes, while it could be as high as 200 mM in halophytes. The regulation of $Na^+$ and $Cl^-$ levels is critical of metabolic processes like photosynthesis (Bose et al. 2017).

*F. indica* (family Zygophyllaceae) is distributed in tropical, subtropical, and warm areas of the world (Kanwal et al. 2017)). It primarily colonizes arid saline regions throughout Pakistan, even where annual rainfall is as low as 60 mm. *F. indica* dominates saline patches and inter-dune areas in the Cholistan Desert. This species has a good potential for phytoremediation of metal-contaminated soils (Alsihany et al. 2019), especially having high accumulation coefficient for Cr, Ni, and Cu (Ghoneim et al. 2014). Being a xerohalophyte (Khan and Qaiser 2006), this species is expected to have good potential for the phytoremediation of saline/sodic soils. It is also a medicinally very important species used to cure hematological, neurological, endocrinological, and inflammatory disorders. It is a blood purifier and possesses deobstruent properties. It is also used for skin diseases, smallpox, and snake bites and applied externally on tumors (Satpute et al. 2012

Keeping in view of the ability of the *F. indica* to maintain dense stands while growing in hypersaline soils, it was worth studying the specific modifications for salinity tolerance in its differently adapted populations. Moreover, the role of morphological, anatomical, and biochemical attributes towards its phytoremediation potential needs to be explored. It was hypothesized that the phytoremediation potential of *F. indica* in these hypersaline arid environments must be linked with variable eco-physiological, morphological, and anatomical adaptive features. Differential phytoremediation potential of different populations might correspond to a specific set of environmental conditions in which populations of *F. indica* are growing. In the current study, key physio-anatomical phytoremediation components specific to different *F. indica* populations were examined. The following research questions were addressed: (a) whether variation in phytoremediation-related structural and functional features existed among different populations of *F. indica?* (b) If yes, then how these variations are beneficial for the remediation of hypersaline soils using different populations of *F. indica*?

## Material and methods

### Study area

Cholistan desert, the seventh-largest desert in the world, is located in Punjab province (coordinates: 27°42′00.71 to 29°07′09.8″N, 70°52′05.82″ to 69°55′01.82″, average elevation: 112 m a.s.l.). It receives very low precipitation of less than 100 mm in deep desert and around 200 mm around the edges. Temperature ranges from 6.5 to 46.5 °C, but in summer, the maximum temperature may rise to 50 °C or above with relative humidity of less than 30% in most of the area. This makes Cholistan extremely hot, dry, and saline desert with limited vegetation.

### Collection sites

Four populations of *F. indica* (each with three replications) were collected from different areas of the lesser Cholistan

Desert to evaluate their eco-morphological and anatomical adaptations. Study sites were located at a distance of about 60 km from each other. Study sites from the least to the highest salinity include Derawar Fort, Traway Wala Toba, Ladam Sir (Ladam Sir), and Pati Sir (PS).

## Ecological traits

For ecological traits, four locations (replications) were selected at each site at 500 m. At each location, a primary transect was laid out in a 200-m area, and then 10 sub-transects (of 210 m length) were laid out perpendicularly at 20 m from each other. Ten quadrats (of 1 m × m) were laid out regularly at 10 m on sub-transects. Ten quadrats were randomly selected for morphological and anatomical traits, whereas for ecological studies, data from all 100 quadrates were recorded at each study site (Fig. 1).

## Soil physicochemical characters

Rhizospheric soil samples were taken at the depth of 15 cm from all ten quadrats, mixed thoroughly, and used for analyzing soil physicochemical characters. Fresh soil samples were weighed with a digital balance and oven-dried at 70 °C until a constant weight was achieved. Moisture contents were calculated as the difference between fresh and dry weights of the soil samples. Soil saturation percentage was determined in accordance with Richards (1954). Organic matter in soil was measured by following the method of Sims and Haby (1971). A soil saturation paste was prepared, and soil water was extracted by a vacuum pump. Soil ECe and pH were measured with an ECe/pH meter (Ino LAB pH/Cond 720, WTW series). The soil ionic contents ($Na^+$, $K^+$, and $Ca^{2+}$) were measured with a flame photometer (PFP–7, Jenway, Staffordshire, UK). A digital chloride meter was used to determine the $Cl^-$ concentration (Model 926, Sherwood Scientific

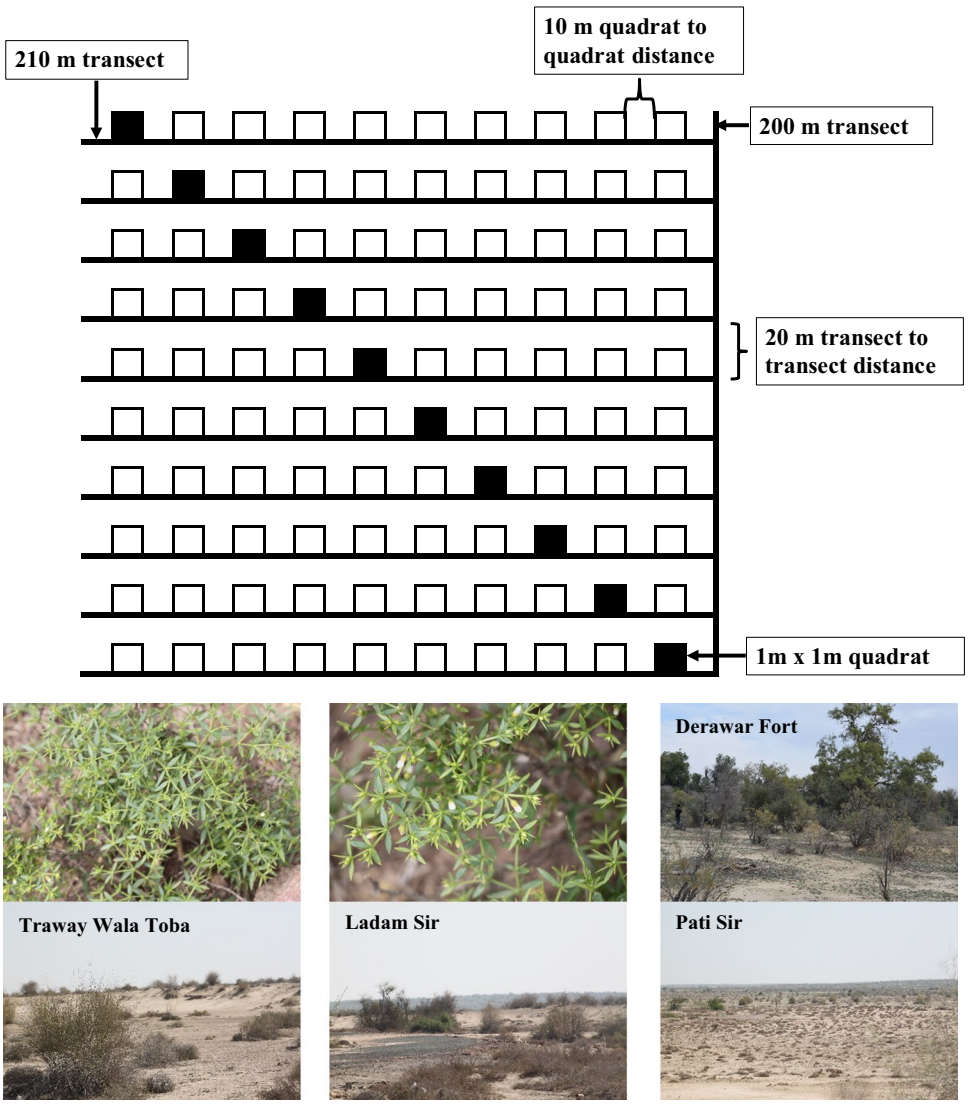


**Fig. 1** Layout of vegetation sampling, plant habit, and collection sites in the Cholistan Desert. Black squares indicated the quadrats selected for plant material collection and soil sampling

Ltd., Cambridge, UK). Soil $Mg^{2+}$ was estimated by an atomic absorption spectrophotometer (Analyst 3000, Perkin Elmer, Rodgau, Germany). Soil $PO_4^{3-}$ was determined spectrophotometrically by following the method of Yoshida et al. (1971) while $NO_3^-$ according to the method of Kowalenko and Lowe (1973).

## Plant analysis and measurements

### Morphological characteristics

Plants were uprooted carefully with the help of plant auger (20 cm dia.) and washed gently in a water cooler keeping in view of the minimum damage to the roots. Root and shoot (aboveground plant organs) fresh weights were taken immediately after uprooting the plant with a portable digital balance, while dry weights were measured later in the laboratory after properly drying the material for 1 week at 60 °C. The root and shoot lengths were recorded with a measuring scale. Leaf area was measured by using a formula devised by Schrader et al. (2021).

$$\text{Leaf area} = \text{Length} \times \text{Width} \times \text{correction factor } 0.69$$

### Root and shoot ionic content

Plant material was acid digested by the method of Wolf (1982) and used for the determination of shoot (aboveground plant organs) and root $Ca^{2+}$, $K^+$, and $Na^+$ concentrations using a flame photometer (Jenway, PFP–7, UK). A digital chloride meter was used to determine the concentration of $Cl^-$ concentration (Model 926, Sherwood Scientific Ltd., Cambridge, UK). Root and shoot $Mg^{2+}$ was estimated by an atomic spectrophotometer (Perkin Elmer, Analyst 300). Plant $PO_4^{3-}$ was determined using UV–visible spectrophotometer (Hitachi 220, Japan spectrophotometrically (Hitachi 220, Japan) following the method of Yoshida et al. (1971) while $NO_3^-$ according to the method of Kowalenko and Lowe (1973).

### Excreted ions

The topmost 10 leaves were selected from the longest branch of each plant were selected for ion excretion. The leaves were washed in 50 ml of distilled water with a gentle brushing. The extracted ions ($Na^+$, $K^+$, $Ca^{2+}$, $Mg^{2+}$, $PO_4^{3-}$, $NO_3^-$, and $Cl^-$) were determined following the procedures outlined in the previous section.

### Anatomical traits

Plant material was fixed in formalin acetic alcohol (FAA) for 36 h and transferred to acetic alcohol (Ruzin 1999). Permanent slides were prepared by using the freehand sectioning. A gradual dehydration of plant tissues was performed by a series of ethanol grades. Lignified tissues (xylem vessels and mechanical tissue) were stained with safranin while parenchymatous tissue and phloem with fast green. An ocular micrometer was calibrated with a stage micrometer, and different anatomical measurements were taken on a compound stereomicroscope (Nikon 104, Tokyo, Japan).

## Phytoremediation traits

The sodium and chloride bioconcentration factors (BCF), translocation factors (TF), dilution factors, and ion excretion efficiency (IEE) were calculated by the following equations (Diwan et al. 2010).

$$\text{Bioconcentration factor} = \frac{\text{Tissue } Na^+ \text{ or } Cl^-(\text{mgkg}^{-1}\text{DW})}{\text{Soil } Na^+ \text{ or } Cl^-(\text{mgkg}^{-1}\text{DW})}$$

$$\text{Translocation factor} = \frac{\text{Shoot } Na^+ \text{ or } Cl^-(\text{mgkg}^{-1}\text{DW})}{\text{Root } Na^+ \text{ or } Cl^-(\text{mgkg}^{-1}\text{DW})}$$

$$\textit{Dilution factor} = \textit{Root or shoot BCF x root or shoot dry weight x } 100$$

$$\text{Ion excretion efficiency} = \frac{\text{Excreted } Na^+(\text{mgL}^{-1}\text{DW})}{\text{Shoot } Na^+(\text{mgkg}^{-1}\text{DW})}$$

## Statistical analysis

Data were subjected to an analysis of variance (ANOVA) using completely randomized design with three replications. *F*-test was performed to check significance of various variables, which was followed by the least significant difference (LSD) test for the comparison of means ($P > 0.05$) (Minitab, LLC, State College, PA, USA). The data were subjected to the multivariate redundancy analysis (RDA) to determine possible link between the traits studied, and a response curve was generated by fitting a generalized linear model (GLM) in CANOCO (Version 5 for Windows).

# Results

## Environmental and soil physicochemical characters

Average temperature remained consistent at all study sites, while annual rainfall was significantly higher at more saline LS (Ladam Sir) and Pati Sir (Patti Sir) sites. Soil saturation percentage, moisture contents, ECe, $Na^+$,

$Cl^-$, $NO_3^-$, and $PO_4^{3-}$ were the highest at the Pati Sir site. Organic matter was the highest at the Ladam Sir site. The pH was more basic at the Derawar Fort site (Table 1).

## Eco-morphological traits

Analysis of variance (*F*-ratios and *p*-values) are summarized in Table 2. Relative frequency was the greatest (0.7) at the Pati Sir and Traway Wala Toba 0.6) sites while the lowest (0.1) at the Derawar Fort site. Relative density (3.5), cover (5.6), and importance values (1.7) were the highest at the Ladam Sir site. Morphological traits such as leaf area and root and shoot lengths were the maximum in plants collected from the Derawar Fort site (Tables 2 and 3), while the lowest of all morphological traits were observed in plants from the highest saline Pati Sir site.

## Root and shoot ionic content

Shoot and root $K^+$, $Na^+$, and $Cl^-$ and shoot $Mg^{2+}$ and $Ca^{2+}$ were the highest in the plants from Pati Sir site. Plants from the Ladam Sir site accumulated the most root $Ca^{2+}$ and root $PO_4^{3-}$. Plant from the Traway Wala Toba site had the maximum concentration of root $Mg^{2+}$. The root and shoot $NO_3^-$ ions were the greatest in plants from the Derawar Fort site (Tables 2 and 3).

## Excreted ions

Plants from the Pati Sir site excreted the highest concentration of $Na^+$, $K^+$, and $PO_4^{3-}$. Excretion of $Mg^{2+}$ and $Ca^{2+}$ was the highest in plants from the Ladam Sir and PS site, while plants from the Derawar Fort site excreted the highest concentration of $NO_3^-$ (Table 2 and 3).

## Anatomical traits

### Root anatomical traits

The thickest roots (2.4 $mm^2$) were recorded in the Pati Sir population while the thinnest (1.1 $mm^2$) in the Derawar Fort population. Exodermal and hypodermal cell area generally increased with increase in the salinity level of the habitats. Exodermis was the maximum (645.5 $\mu m^2$) in the Pati Sir population whereas hypodermis (575.9 $\mu m^2$) the maximum in the Ladam Sir population. The largest cortical cells (4010.9 $\mu m^2$) were seen in the Ladam Sir population, while the Pati Sir population possessed the thickest (350.8 µm) cortical region. A significant reduction (78.8 µm) in cortical thickness was recorded in the Derawar Fort population, while the smallest cortical cells (2301.6 $\mu m^2$) were seen in the Traway Wala Toba population. The largest endodermal cells (1377.9 $\mu m^2$) were observed in the Pati Sir population and pericycle cells in the Ladam Sir population (366.2 $\mu m^2$). Endodermal cell area was the minimum (470.6 $\mu m^2$), while the shortest

**Table 1** Soil physicochemical characteristics of the collection sites of *Fagonia indica* in the Cholistan Desert

| Characteristics | Collection sites | | | | LSD |
|---|---|---|---|---|---|
| | Derawar Fort | Traway Wala Toba | Ladam Sir | Pati Sir | |
| Weather | | | | | |
| Annual rainfall (mm) | 80.2c | 93.4b | 98.9a | 96.6a | 3.5* |
| Minimum mean temperature (°C) | 0 | 1 | 1 | 1 | 2.1NS |
| Maximum mean temperature (°C) | 50 | 49 | 49 | 48 | 2.3NS |
| Soil properties | | | | | |
| Saturation percentage (%) | 18c | 24b | 23b | 28a | 1.9* |
| Moisture content (%) | 15b | 17.3b | 16.3b | 20.1a | 2.5* |
| Organic matter (%) | 0.7bc | 0.8ab | 0.9a | 0.6c | 1.3* |
| Soil pH | 9.7a | 7.2c | 8.4b | 8.1b | 0.7* |
| ECe (dS $m^{-1}$) | 21d | 32c | 39b | 51a | 4.9** |
| Soil $Na^+$ (mg $kg^{-1}$) | 3774d | 4189c | 4556b | 5312a | 216.3** |
| Soil $K^+$ (mg $kg^{-1}$) | 312b | 363a | 271d | 280c | 6.9** |
| Soil $Ca^{2+}$ (mg $kg^{-1}$) | 66b | 73a | 59c | 60c | 3.4** |
| Soil $Mg^{2+}$ (mg $kg^{-1}$) | 0.54b | 0.63a | 0.32c | 0.32c | 0.04** |
| Soil $Cl^-$ (mg $kg^{-1}$) | 1685d | 2481c | 2617b | 2713a | 76.5** |
| Soil $NO_3^-$ (mg $kg^{-1}$) | 2.4c | 2.6bc | 2.8b | 3.1a | 2.2* |
| Soil $PO_4^{3-}$ (mg $kg^{-1}$) | 3.11c | 2.45b | 2.32b | 3.96a | 0.6** |

*NS* not significant, *significant at $p \geq 0.05$, **significant at $p \geq 0.01$

**Table 2** One-way analysis of variance showing F-ratio and *p*-values of different variables of *Fagonia indica* in the Cholistan Desert (*df* = 3)

| Variable | F-ratio | *p*-value | Variable | F-ratio | *p*-value |
|---|---|---|---|---|---|
| Ecology | | | | | |
| Relative frequency | 16.30 | 0.0009*** | Relative density | 93.08 | 0.0000*** |
| Relative cover | 274.53 | 0.0000*** | Importance value | 18.22 | 0.0006*** |
| Morphology | | | | | |
| Total leaf area | 364.66 | 0.0000*** | Root length | 1073.20 | 0.0000*** |
| Shoot length | 963.82 | 0.0000*** | | | |
| Ionic content | | | | | |
| Shoot $Na^+$ | 24,912.65 | 0.0000*** | Root $Na^+$ | 28,874.30 | 0.0000*** |
| Shoot $K^+$ | 9157.29 | 0.0000*** | Root $K^+$ | 18,893.91 | 0.0000*** |
| Shoot $Ca^{2+}$ | 215.03 | 0.0000*** | Root $Ca^{2+}$ | 642.33 | 0.0000*** |
| Shoot $Cl^-$ | 147,788.2 | 0.0000*** | Root $Cl^-$ | 166,760.78 | 0.0000*** |
| Shoot $Mg^{2+}$ | 2.94 | 0.0989 ns | Root $Mg^{2+}$ | 8.22 | 0.0079** |
| Shoot $PO_4^{3-}$ | 2592.18 | 0.0000*** | Root $PO_4^{3-}$ | 96,256.72 | 0.0000*** |
| Shoot $NO_3^-$ | 7.27 | 0.0113* | Root $NO_3^-$ | 16.94 | 0.0008*** |
| Excreted ions | | | | 0 | |
| Excreted $Na^+$ | 2511.75 | 0.0000*** | Excreted $K^+$ | 265.29 | 0.0000*** |
| Excreted $Ca^{2+}$ | 2170.54 | 0.0000*** | Excreted $Cl^-$ | 883.57 | 0.0000*** |
| Excreted $Mg^{2+}$ | 13.38 | 0.0017** | Excreted $PO_4^{3-}$ | 49.17 | 0.0000*** |
| Excreted $NO_3^-$ | 11.63 | 0.0027** | | | |
| Root anatomy | | | | | |
| Root cross-sectional area | 32.11 | 0.0001*** | Exodermal cell area | 2,104,256.7 | 0.0000*** |
| Hypodermal cell area | 184,388.53 | 0.0000*** | Cortical thickness | 46,190.43 | 0.0000*** |
| Cortical cell area | 72,966,280 | 0.0000*** | Endodermal cell area | 25,418,774 | 0.0000*** |
| Pericycle cell area | 197,529.44 | 0.0000*** | Metaxylem area | 16,225,390 | 0.0000*** |
| Phloem area | 69,018,111 | 0.0000*** | | | |
| Stem anatomy | | | | | |
| Stem cross-sectional area | 10.70 | 0.0036** | Epidermal cell area | 10,608,380 | 0.0000*** |
| Hypodermal cell area | 27,323,196 | 0.0000*** | Cortical thickness | 112,842.76 | 0.0000*** |
| Cortical cell area | 25,459,480 | 0.0000*** | Metaxylem area | 10,047,980 | 0.0000*** |
| Phloem area | 15,661,890 | 0.0000*** | Pith thickness | 6,077,509.2 | 0.0000*** |
| Pith cell area | 14,014,683 | 0.0000*** | Sclerenchymatous cell area | 26,611,590 | 0.0000*** |
| Leaf anatomy | | | | | |
| Midrib thickness | 209,432.59 | 0.0000*** | Lamina thickness | 159,675.22 | 0.0000*** |
| Abaxial epidermal cell area | 112,237.81 | 0.0000*** | Adaxial epidermal cell area | 365,596.54 | 0.0000*** |
| Abaxial stomatal density | 3905.01 | 0.0000*** | Adaxial stomatal density | 9295.15 | 0.0000*** |
| Abaxial stomatal area | 1462.98 | 0.0000*** | Adaxial stomatal area | 2538.56 | 0.0000*** |
| Parenchymatous cell area | 13,515,894 | 0.0000*** | Palisade cell area | 353,598.8 | 0.0000*** |
| Spongy cell area | 7820.47 | 0.0000*** | Metaxylem area | 62,054,455 | 0.0000*** |
| Phloem area | 11,922,380 | 0.0000*** | Salt gland density | 4841.80 | 0.0000*** |
| Salt gland area | 5765.41 | 0.0000*** | | | |

*Significant at $p > 0.05$, **significant at $p > 0.01$, ***significant at $p > 0.001$, *ns* not significant

(279.3 $\mu m^2$) pericycle cells were seen in the Derawar Fort population. The Traway Wala Toba and Pati Sir populations exhibited the broadest metaxylem vessels (20,142.4 and 20,054.5 $\mu m^2$, respectively). Phloem area was the highest (11,649.1 $\mu m^2$), while the lowest (9469.2 $\mu m^2$) of it was recorded in the Pati Sir population (Tables 2 and 4, Fig. 2).

### Stem anatomical traits

Stem cross-sectional area was the largest (1.9 $mm^2$) in the Pati Sir population, whereas the thinnest (1.1 $mm^2$) cross-sectional area was noticed in the Derawar Fort population. The largest (2755.8 $\mu m^2$) epidermal cells were observed in the Derawar Fort population and the smallest 749.6 $\mu m^2$)

**Table 3** Eco-morphological characteristics of differently adapted *Fagonia indica* populations in the Cholistan Desert

| Characteristics | Collection sites | | | | LSD |
|---|---|---|---|---|---|
| | Derawar Fort | Traway Wala Toba | Ladam Sir | Pati Sir | |
| Ecology | | | | | |
| Relative frequency | 0.1b | 0.6a | 0.3b | 0.7a | 1.3NS |
| Relative density | 1.2b | 1.7b | 3.5a | 3.3a | 0.8NS |
| Relative cover | 1.9c | 4.0b | 5.6a | 4.7ab | 0.9* |
| Importance value | 3.2d | 6.3c | 9.4a | 8.7b | 0.4** |
| Morphology | | | | | |
| Total leaf area ($cm^2$ $plant^{-1}$) | 6.4a | 4.1b | 2.2c | 1.3d | 0.6** |
| Root length (cm) | 17.5a | 12.8b | 16.5a | 9.7c | 2.3** |
| Shoot length (cm) | 17.9a | 15.8b | 12.5c | 10.1d | 1.3** |
| Ionic content | | | | | |
| Shoot $Na^+$ (mg $g^{-1}$ d.w.) | 57.7d | 69.6c | 88.5b | 95.3a | 4.6** |
| Root $Na^+$ (mg $g^{-1}$ d.w.) | 47.0c | 51.2c | 73.4b | 85.1a | 5.2** |
| Shoot $K^+$ (mg $g^{-1}$ d.w.) | 28.4c | 33.3bc | 39.9b | 51.4a | 6.3** |
| Root $K^+$ (mg $g^{-1}$ d.w.) | 13.5d | 17.3c | 28.4b | 43.2a | 3.6** |
| Shoot $Ca^{2+}$ (mg $g^{-1}$ d.w.) | 4.6b | 6.2ab | 7.3a | 7.7a | 0.6* |
| Root $Ca^{2+}$ (mg $g^{-1}$ d.w.) | 2.2d | 3.6c | 7.5a | 4.9b | 1.2** |
| Shoot $Cl^-$ (mg $g^{-1}$ d.w.) | 19.4d | 46.3c | 73.5b | 92.8a | 21.7** |
| Root $Cl^-$ (mg $g^{-1}$ d.w.) | 20.4d | 52.9c | 87.5b | 91.7a | 2.8** |
| Shoot $Mg^{2+}$ (mg $g^{-1}$ d.w.) | 0.5c | 0.7b | 0.8ab | 0.9a | 1.3* |
| Root $Mg^{2+}$ (mg $g^{-1}$ d.w.) | 0.4c | 0.9a | 0.6b | 0.3c | 1.4* |
| Shoot $PO_4^{3-}$ (mg $g^{-1}$ d.w.) | 72.7d | 82.3b | 85.6a | 75.9c | 1.6** |
| Root $PO_4^{3-}$ (mg $g^{-1}$ d.w.) | 26.0c | 92.3a | 93.2a | 80.6b | 2.6** |
| Shoot $NO_3^-$ (mg $g^{-1}$ d.w.) | 2.7a | 2.4b | 2.3b | 1.9c | 0.2* |
| Root $NO_3^-$ (mg $g^{-1}$ d.w.) | 3.2a | 3.1a | 2.5b | 2.1b | 0.5* |
| Excreted ions | | | | | |
| Excreted $Na^+$ (mg $L^{-1}$) | 16.2c | 15.3c | 21.1b | 25.6a | 2.7** |
| Excreted $K^+$ (mg $L^{-1}$) | 7.3a | 5.1b | 3.7c | 6.4a | 1.1* |
| Excreted $Ca^{2+}$ (mg $L^{-1}$) | 21.5b | 17.1c | 27.8a | 25.2a | 3.1** |
| Excreted $Cl^-$ (mg $L^{-1}$) | 12.4b | 9.6c | 16.3a | 9.2c | 0.8** |
| Excreted $Mg^{2+}$ (mg $L^{-1}$) | 0.9a | 0.3b | 0.7a | 0.8a | 0.3* |
| Excreted $PO_4^{3-}$ (mg $L^{-1}$) | 1.1b | 0.5c | 1.8a | 1.9a | 0.2** |
| Excreted $NO_3^-$ (mg $L^{-1}$) | 1.5a | 1.3ab | 1.2b | 0.8c | 0.3* |

Means sharing different alphabets are statistically significant at $p \geq 0.05$. *NS* not significant, *significant at $p \geq 0.05$, **significant at $p \geq 0.01$

in the Pati Sir population (Tables 2 and 4). The Ladam Sir population possessed the maximum (1970.2 $\mu m^2$) hypodermal cell area, while Pati Sir had the minimum 994.3 $\mu m^2$). Cortex thickness, cortical cell area, metaxylem area, and phloem area were the maximum in the Traway Wala Toba population, measuring to 157.6, 4446.7, 7097.7 and 15,172.8 $\mu m^2$, respectively. Pith thickness (854.3 µm), pith cell area (1150.9 $\mu m^2$), and sclerenchyma bundle area (10,201.7 $\mu m^2$) were the maximum in the Pati Sir population (Fig. 2).

### Leaf blade anatomy

Abaxial stomatal number was the highest (35.8 per $mm^2$) in the Traway Wala Toba population, closely followed the Pati Sir population (33.6 per $mm^2$). Adaxial stomatal density was the maximum in the Ladam Sir population (40.6 per $mm^2$), while the minimum (19.5 per $mm^2$) in the Derawar Fort population (Tables 2 and 4, Fig. 3). The largest stomata on abaxial and adaxial epidermal surfaces were noted in the Derawar Fort population, measured as 17.6 and 16.3 $\mu m^2$, respectively. Leaf anatomical traits like midrib thickness (462.4 µm), lamina thickness (369.2 µm), abaxial epidermal cell area (139.1 $\mu m^2$), parenchymatous thickness (184.9 µm) and cell area (1220.4 $\mu m^2$), palisade (976.9 $\mu m^2$) and spongy cell area (122.7 $\mu m^2$), metaxylem area (4935.2 $\mu m^2$), and phloem area (3575.5 $\mu m^2$) were the maximum in the Traway Wala Toba populations. The largest adaxial epidermal cells (331.4 $\mu m^2$) were noted in the Pati Sir population, while the

**Table 4** Root, stem, and leaf anatomical characteristics of differently adapted *Fagonia indica* populations in the Cholistan Desert

| Characteristics | Collection sites | | | | LSD |
|---|---|---|---|---|---|
| | Derawar Fort | Traway Wala Toba | Ladam Sir | Pati Sir | |
| Root anatomy | | | | | |
| Root cross-sectional area ($mm^2$) | 1.1c | 1.6b | 1.9b | 2.4a | 0.4** |
| Exodermal cell area ($\mu m^2$) | 348.8c | 313.9d | 453.4b | 645.5a | 21.8** |
| Hypodermal cell area ($\mu m^2$) | 453.4b | 348.8d | 575.9a | 401.1c | 32.7** |
| Cortical thickness (μm) | 323.8b | 307.6c | 342.2a | 350.8a | 10.4** |
| Cortical cell area ($\mu m^2$) | 2336.4c | 2301.6c | 4010.9a | 3243.7b | 43.9** |
| Endodermal cell area ($\mu m^2$) | 505.3c | 749.8b | 470.6d | 1377.9a | 21.3** |
| Pericycle cell area ($\mu m^2$) | 279.3d | 331.4b | 366.2a | 313.0c | 11.5** |
| Metaxylem area ($\mu m^2$) | 13,375.8b | 20,142.4a | 13,462.7b | 20,054.5a | 216.2** |
| Phloem area ($\mu m^2$) | 10,289.7b | 11,649.1a | 10,725.4b | 9469.2c | 521.8** |
| Stem anatomy | | | | | |
| Stem cross-sectional area ($mm^2$) | 1.1c | 1.7ab | 1.5b | 1.9a | 2.3* |
| Epidermal cell area ($\mu m^2$) | 2755.8a | 1081.2b | 1063.7b | 749.6c | 31.7** |
| Hypodermal cell area ($\mu m^2$) | 1552.8b | 1046.5c | 1970.2a | 994.3d | 35.6** |
| Cortical thickness (μm) | 78.8c | 157.6a | 144.1a | 106.7b | 21.3** |
| Cortical cell area ($\mu m^2$) | 3906.6b | 4446.7a | 1046.5d | 2476.3c | 206.1** |
| Metaxylem area ($\mu m^2$) | 5231.3b | 7097.7a | 4621.6c | 2406.9d | 322.7** |
| Phloem area ($\mu m^2$) | 13,864.7b | 15,172.8a | 5876.9d | 12,224.3c | 1097.4** |
| Pith thickness (μm) | 582.8c | 277.4c | 598.7b | 854.3a | 6.8** |
| Pith cell area ($\mu m^2$) | 348.8c | 383.6b | 279.3d | 1150.9a | 23.6** |
| Sclerenchymatous cell area ($\mu m^2$) | Absent | 10,097.3a | 7062.8b | 10,201.7a | 311.4** |
| Leaf anatomy | | | | | |
| Abaxial stomatal density per $mm^2$ | 23.3c | 35.8a | 28.3b | 33.6a | 3.1* |
| Adaxial stomatal density per $mm^2$ | 19.5c | 26.7b | 40.6a | 27.4b | 4.6** |
| Abaxial stomatal area ($\mu m^2$) | 17.6a | 11.4b | 9.2b | 10.9b | 4.1* |
| Adaxial stomatal area ($\mu m^2$) | 16.3a | 5.4c | 12.9b | 6.6c | 2.8** |
| Midrib thickness (μm) | 353.6c | 462.4a | 413.5b | 359.2c | 11.7** |
| Lamina thickness (μm) | 293.7c | 369.2a | 282.8d | 304.4b | 6.5** |
| Abaxial epidermal cell area ($\mu m^2$) | 69.6c | 139.1a | 63.7c | 104.2b | 11.5** |
| Adaxial epidermal cell area ($\mu m^2$) | 296.6c | 209.2d | 313.9b | 331.4a | 12.2** |
| Parenchymatous cell area ($\mu m^2$) | 1098.7b | 1220.4a | 627.8d | 784.5c | 104.3** |
| Palisade cell area ($\mu m^2$) | 802.2b | 976.9a | 819.4b | 749.8c | 25.3** |
| Spongy cell area ($\mu m^2$) | 104.3b | 122.7a | 105.2b | 109.6b | 9.2* |
| Metaxylem area ($\mu m^2$) | 1865.9d | 4935.2a | 2040.3c | 2999.5b | 35.8** |
| Phloem area ($\mu m^2$) | 1028.1d | 3575.5a | 1639.7b | 1517.2c | 73.9** |
| Salt gland density per $mm^2$ | 3.2d | 8.3c | 12.8b | 18.9a | 1.4** |
| Salt gland area ($\mu m^2$) | 12.3b | 18.4a | 4.2c | 3.1c | 2.1** |

Means sharing different alphabets are statistically significant at $p \geq 0.05$. *Significant at $p \geq 0.05$, **significant at $p \geq 0.01$

smallest (209.2 $\mu m^2$) was noted in the Traway Wala Toba population (Table 3, Fig. 2).

Adaxial stomatal density increased with increase in salinity level of the habitats. Stomatal density was the maximum in Traway Wala Toba population, which thereafter decreased with increase in salinity levels. The stomatal area decreased along increasing salinity gradient on both leaf surfaces, where the abaxial surface was relatively more affected at the highest salinity (Pati Sir site). Salt gland density increased significantly along salinity levels, whereas salt gland area responded otherwise, i.e., decreased with salinity level (Tables 2 and 4, Fig. 3).

## Phytoremediation traits

Root $Na^+$ and root and shoot $Cl^-$ bioconcentration factor were the highest in the Pati Sir population, while shoot $Na^+$ bioconcentration factor was the maximum in the Ladam

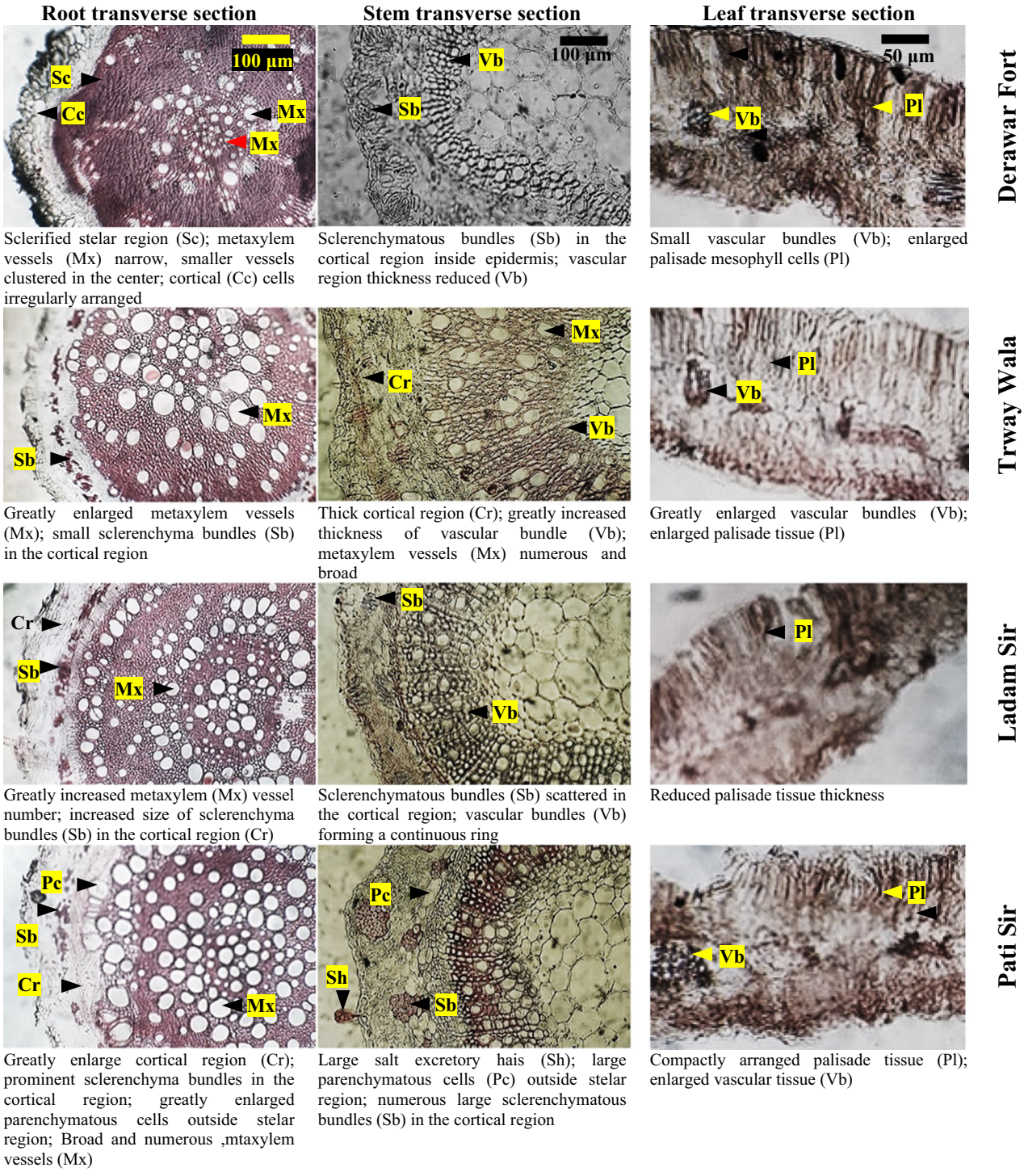


**Fig. 2** Root, stem, and leaf transverse sections of *Fagonia indica* collected from extremely hot arid and saline conditions of the Cholistan Desert

Sir population. The lowest root and shoot $Na^+$ and $Cl^-$ bioconcentration factor were recorded in the Derawar Fort population (Table 5). The greatest root to shoot $Na^+$ translocation factor was seen in the Traway Wala Toba population, whereas root to shoot $Cl^-$ translocation factor was high in Pati Sir population. Ion excretion efficiency was the maximum in the Derawar Fort population, while the minimum was observed in the Traway Wala Toba population. Root and shoot $Na^+$ and $Cl^-$ dilution factor were the highest in the Ladam Sir population, whereas shoot $Cl^-$ dilution factor was the maximum in the Pati Sir population. Root and shoot $Cl^-$ dilution factor was the lowest in the Derawar Fort

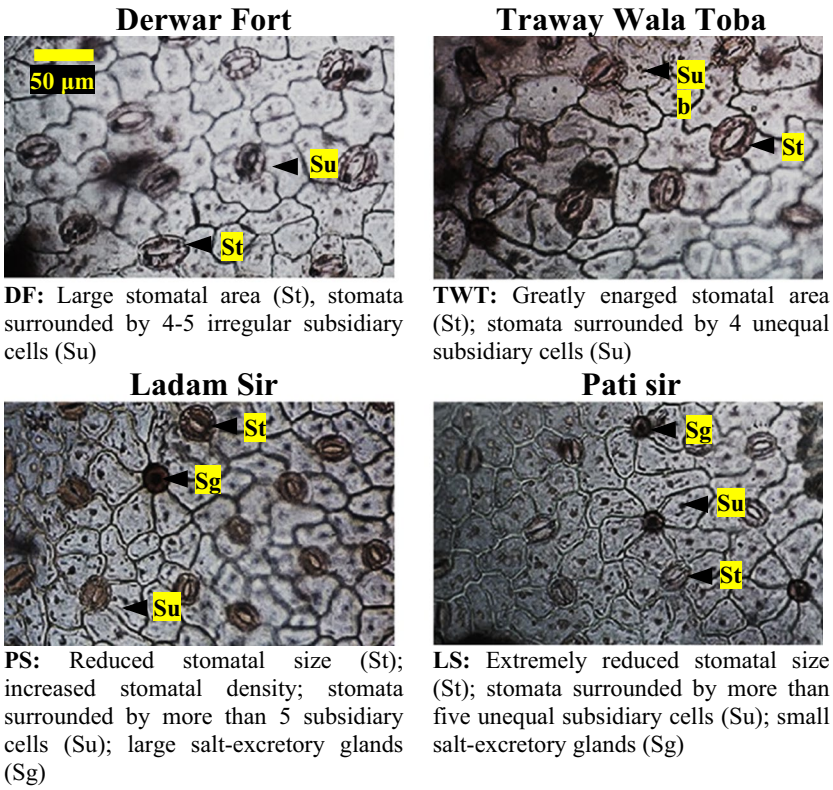


**DF:** Large stomatal area (St), stomata surrounded by 4-5 irregular subsidiary cells (Su)

**TWT:** Greatly enarged stomatal area (St); stomata surrounded by 4 unequal subsidiary cells (Su)

**PS:** Reduced stomatal size (St); increased stomatal density; stomata surrounded by more than 5 subsidiary cells (Su); large salt-excretory glands (Sg)

**LS:** Extremely reduced stomatal size (St); stomata surrounded by more than five unequal subsidiary cells (Su); small salt-excretory glands (Sg)

**Fig. 3** Leaf epidermal surface of *Fagonia indica* collected from the Cholistan Desert. *DF*, large stomatal area (St), stomata surrounded by 4–5 irregular subsidiary cells (Su). *TWT*, greatly enlarged stomatal area (St); stomata surrounded by 4 unequal subsidiary cells (Su). *PS*, reduced stomatal size (St); increased stomatal density; stomata surrounded by more than 5 subsidiary cells (Su); large salt-excretory glands (Sg). *LS*, extremely reduced stomatal size (St); stomata surrounded by more than five unequal subsidiary cells (Su); small salt-excretory glands (Sg)

population. Root $Na^+$ dilution factor was the minimum in the Traway Wala Toba population, while shoot $Na^+$ dilution factor was high in the Pati Sir population (Table 5).

## Redundancy analysis

Soil $K^+$, $Ca^{2+}$, and $Mg^{2+}$ influenced $Na^+$ and $Cl^-$ translocation factor in the Traway Wala Toba population, which in turn showed association with relative frequency and shoot length (Fig. 4 a). The maximum mean temperature was strongly related to ion excretion efficiency, root $Na^+$ and $Cl^-$ bioconcentration factor, and shoot $Na^+$ bioconcentration factor in the Derawar Fort population, which was grouped with total leaf area. Root $Cl^-$ dilution factor and shoot $Na^+$ dilution factor was influenced by the minimum mean temperature, annual rainfall, soil ECe, moisture content, saturation percentage, and $Na^+$, $Cl^-$, and $NO_3^-$ in the Pati Sir population, which showed association with relative density and relative frequency. Root $Na^+$ dilution factor was influenced by soil organic matter and soil pH of the study sites.

**Table 5** Phytoremediation characteristics of differently adapted *Fagonia indica* populations in the Cholistan Desert

| Characteristics | Collection sites | | | |
|---|---|---|---|---|
| | Derawar Fort | Traway Wala Toba | Ladam Sir | Pati Sir |
| Root $Na^+$ bioconcentration factor | 0.012 | 0.012 | 0.016 | 0.016 |
| Root $Cl^-$ bioconcentration factor | 0.012 | 0.021 | 0.033 | 0.034 |
| Shoot $Na^+$ bioconcentration factor | 0.015 | 0.017 | 0.019 | 0.018 |
| Shoot $Cl^-$ bioconcentration factor | 0.012 | 0.019 | 0.028 | 0.034 |
| $Na^+$ root-to-shoot translocation factor | 1.228 | 1.359 | 1.206 | 1.120 |
| $Cl^-$ root-to-shoot translocation factor | 0.951 | 0.875 | 0.840 | 1.012 |
| Ion excretion efficiency | 0.277 | 0.216 | 0.237 | 0.262 |
| Root $Na^+$ dilution factor per dry weight basis | 2.615 | 2.078 | 3.061 | 2.403 |
| Root $Cl^-$ dilution factor per dry weight basis | 2.542 | 3.625 | 6.353 | 5.070 |
| Shoot $Na^+$ dilution factor per dry weight basis | 8.868 | 8.640 | 10.489 | 8.611 |
| Shoot $Cl^-$ dilution factor per dry weight basis | 6.678 | 9.704 | 15.166 | 16.419 |

For root anatomy, all phytoremediation traits were linked to root cross-sectional area, cortical thickness, and pericycle cell area (Fig. 4 b). The minimum mean temperature, annual rainfall, soil ECe, moisture content, saturation percentage, and $Na^+$, $Cl^-$, $NO_3^-$, and $PO_4^{3-}$ in the Pati Sir population influenced root epidermal cell area and exodermal cell area. The Ladam Sir population was associated with cortical cell area and the Derawar Fort population with hypodermal cell area and phloem area. Soil organic matter was closely clustered with stem hypodermal cell area and metaxylem area (Fig. 4 c). All phytoremediation parameters clustered separately but were influenced by stem cross-sectional area, cortical thickness, cortical cell area, and phloem area. In the case of leaf anatomy, the minimum mean temperature, annual rainfall, soil ECe, saturation percentage, and $Na^+$, $K^+$, $Ca^{2+}$, and $NO_3^-$ in the Traway Wala Toba population were associated with leaf stomatal density and area on both leaf surfaces (Fig. 4 d). Soil $Na^+$ and organic matter were linked to the leaf adaxial and abaxial epidermal cell area and metaxylem area of the Pati Sir population. The maximum mean temperature and soil pH influenced midrib and lamina thicknesses, palisade cell area, adaxial epidermal

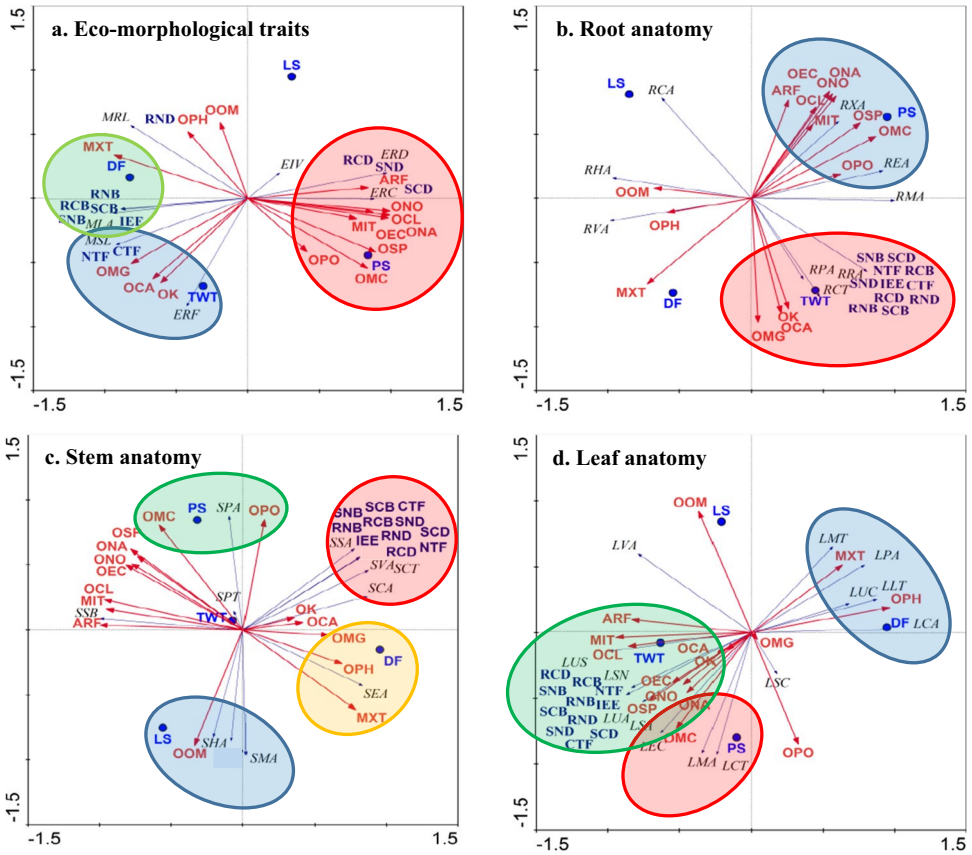


**Fig. 4** Response of soil physicochemical properties on eco-morphological and anatomical traits of *Fagonia indica* collected from the Cholistan Desert. **a** Eco-morphological traits. **b** Root anatomy. **c** Stem anatomy. **d** Leaf anatomy. Collection site: DF, Derawar Fort; TWT, Traway Wala Toba; LS, Ladam Sir; PS, Pati Sir. *Weather*: ARF, annual rainfall; MIT, minimum mean temperature; MXT, maximum mean temperature. *Soil properties*: OPH, soil pH; OEC, soil ECe; ONA, soil $Na^+$; OK, soil $K^+$; OCA, soil $Ca^{2+}$; OMG, soil $Mg^{2+}$; OCL, soil $Cl^-$; ONO, soil $NO_3^-$; OPO, soil $PO_4^{3-}$; OSP, saturation percentage; OMC, moisture content; OOM, organic matter. *Ecology*: ERF, relative density; ERD, relative frequency; EIV, importance value; ERC, relative cover. *Morphology*: MLA, total leaf area; MRL, root length; MSL, shoot length. *Root anatomy*: RRA, root cross-sectional area; RXA, exodermal cell area; RHA, hypodermal cell area; RCT, cortical thickness; RCA, cortical cell area; REA, endodermal cell area; RPA, pericycle cell area; RMA, metaxylem area; RVA, phloem area. *Stem anatomy*: SSA, stem cross-sectional area; SEA, epidermal cell area; SHA, hypodermal cell area; SCT, cortical thickness; SCA, cortical cell area; SMA, metaxylem area; SVA, phloem area; SPT, pith thickness; SPA, pith cell area; SSB, sclerenchyma bundle area. *Leaf anatomy*: LSN, abaxial stomatal density; LUS, adaxial stomatal density; LSA, abaxial stomatal area; LUA, adaxial stomatal area; LMT, midrib thickness; LLT, lamina thickness; LEC, abaxial epidermal cell area; LUC, adaxial epidermal cell area; LCT, adaxial epidermal cell area; LCA, parenchymatous cell area; LPA, palisade cell area; LSC, spongy cell area; LMA, metaxylem area; LVA, phloem area. *Phytoremediation traits*: RNB, root $Na^+$ bioconcentration factor; RCB, root $Cl^-$ bioconcentration factor; RND, root $Na^+$ dilution factor; RCD, root $Cl^-$ dilution factor; SNB, shoot $Na^+$ bioconcentration factor; SCB, shoot $Cl^-$ bioconcentration factor; SND, $Na^+$ dilution factor; SCD, shoot $Cl^-$ dilution factor; NTF, $Na^+$ translocation factor; CTF, $Cl^-$ translocation factor; IEE, ion excretion efficiency

cell area, and parenchymatous cell area in the Derawar Fort population.

For ionic content, shoot $Na^+$ dilution factor and $Na^+$ translocation factor were associated with soil moisture content, $Na^+$, $K^+$, and $Ca^{2+}$ in the Derawar Fort population which influenced excreted $K^+$ and $NO_3^-$ (Fig. 5 a). All phytoremediation traits except shoot $Cl^-$ dilution factor was associated with soil ECe and $Na^+$, which influenced root $Na^+$ and $Ca^{2+}$ and shoot $Ca^{2+}$, $K^+$, $PO_4^{3-}$, and $NO_3^-$ (Fig. 5 b). Shoot $Cl^-$ dilution factor showed a strong association with the maximum mean temperature, soil saturation percentage, moisture content, and $NO_3^-$ in the Pati Sir population, which influenced root $Ca^{2+}$ and $K^+$. The Derawar Fort population was linked to soil $Mg^{2+}$, which influenced shoot $Na^+$ and root shoot $Mg^{2+}$. The Traway Wala Toba population was clustered with soil organic matter, $K^+$ and $Ca^{2+}$, which influenced root and shoot $Cl^-$.

## Response curve

All ecological traits (relative density, relative frequency relative cover, and importance value) showed a positive slope with increasing salinity, while morphological traits (root and shoot length and total leaf area) showed a negative slope (Fig. 6 a). Leaf area was the most adversely affected characteristic. Root anatomical characteristics generally increased with increasing salinity gradient; root cross-sectional area, exodermal cell area, and endodermal cell area showed steeper slope. The response of root hypodermal cell area and phloem area was linear (Fig. 6 b). Stem anatomical parameters like stem cross-sectional area, pith thickness, and its cell area showed steep positive slope along salinity gradient, while cortical thickness weak positively responded. A strong negative slope was recorded in stem traits like cortical cell area and epidermal cell area, while weaker negative response was observed in hypodermal cell area and phloem area. Stem sclerenchymatous bundle area showed a linear response along salinity gradient (Fig. 6 c). A strong negative response was noted in leaf anatomical characteristics like parenchymatous cell area and stomatal area on both leaf surfaces along increasing salinity gradient. Palisade cell area weak negatively responded. A strong positive slope was seen for adaxial epidermal cell area and stomatal density on adaxial and abaxial leaf surface. Leaf features like midrib and lamina thicknesses, spongy cell area, metaxylem area, phloem area, and adaxial epidermal cell area exhibited linear response (Fig. 6 d).

Root and shoot $NO_3^-$ and root $Mg^{2+}$ showed a negative slope along increasing salinity gradient, while all other ionic content (root and shoot $Na^+$, $K^+$, $Ca^{2+}$, $Cl^-$, and shoot $Mg^{2+}$) responded positively (Fig. 7 a). Excreted $NO_3^-$ showed a steep negative slope along increasing salinity gradient, whereas excreted $K^+$ and $Cl^-$ responded weak negatively. A strong positive response was recorded for excreted $Na^+$, $K^+$ and $PO_4^{3-}$ with an increase in salinity level of the habitat, while excreted $Mg^{2+}$ depicted a linear response (Fig. 7 b).

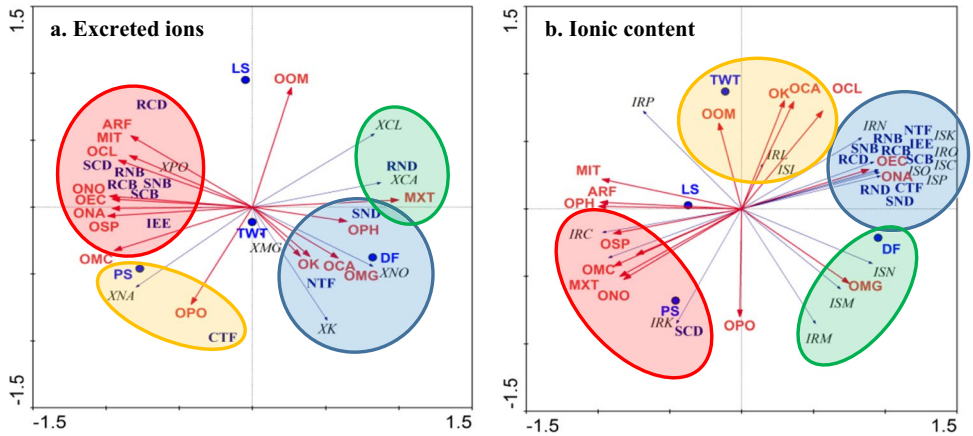


**Fig. 5** Response of soil physicochemical properties on ionic content and excreted ions of *Fagonia indica* collected from the Cholistan Desert. **a** Excreted ions. **b** Ionic content. Collection site: DF, Derawar Fort; TWT, Traway Wala Toba; LS, Ladam Sir; PS, Pati Sir. *Weather*: ARF, annual rainfall; MIT, minimum mean temperature; MXT, maximum mean temperature. *Soil properties*: OPH, soil pH; OEC, soil ECe; ONA, soil $Na^+$; OK, soil $K^+$; OCA, soil $Ca^{2+}$; OMG, soil $Mg^{2+}$; OCL, soil $Cl^-$; ONO, soil $NO_3^-$; OPO, soil $PO_4^{3-}$; OSP, saturation percentage; OMC, moisture content; OOM, organic matter. *Ionic content*: ISN, shoot $Na^+$; IRN, root $Na^+$; ISK, shoot $K^+$; IRK, root $K^+$; ISC, shoot $Ca^{2+}$; IRC, root $Ca^{2+}$; ISL, shoot $Cl^-$; IRL, root $Cl^-$; ISM, shoot $Mg^{2+}$; IRM, root $Mg^{2+}$; ISP, shoot $PO_4^{3-}$; IRP, root $PO_4^{3-}$; ISO, shoot $NO_3^-$; IRO, root $NO_3^-$. *Excreted ions*: XNA, excreted $Na^+$; XK, excreted $K^+$; XCL, excreted $Cl^-$; XPO, excreted $PO_4^{3-}$; XNO, excreted $NO_3^-$; XMG, excreted $Mg^{2+}$; XCA, excreted $Ca^{2+}$. *Phytoremediation traits*: RNB, root $Na^+$ bioconcentration factor; RCB, root $Cl^-$ bioconcentration factor; RND, root $Na^+$ dilution factor; RCD, root $Cl^-$ dilution factor; SNB, shoot $Na^+$ bioconcentration factor; SCB, shoot $Cl^-$ bioconcentration factor; SND, $Na^+$ dilution factor; SCD, shoot $Cl^-$ dilution factor; NTF, $Na^+$ translocation factor; CTF, $Cl^-$ translocation factor; IEE, ion excretion efficiency

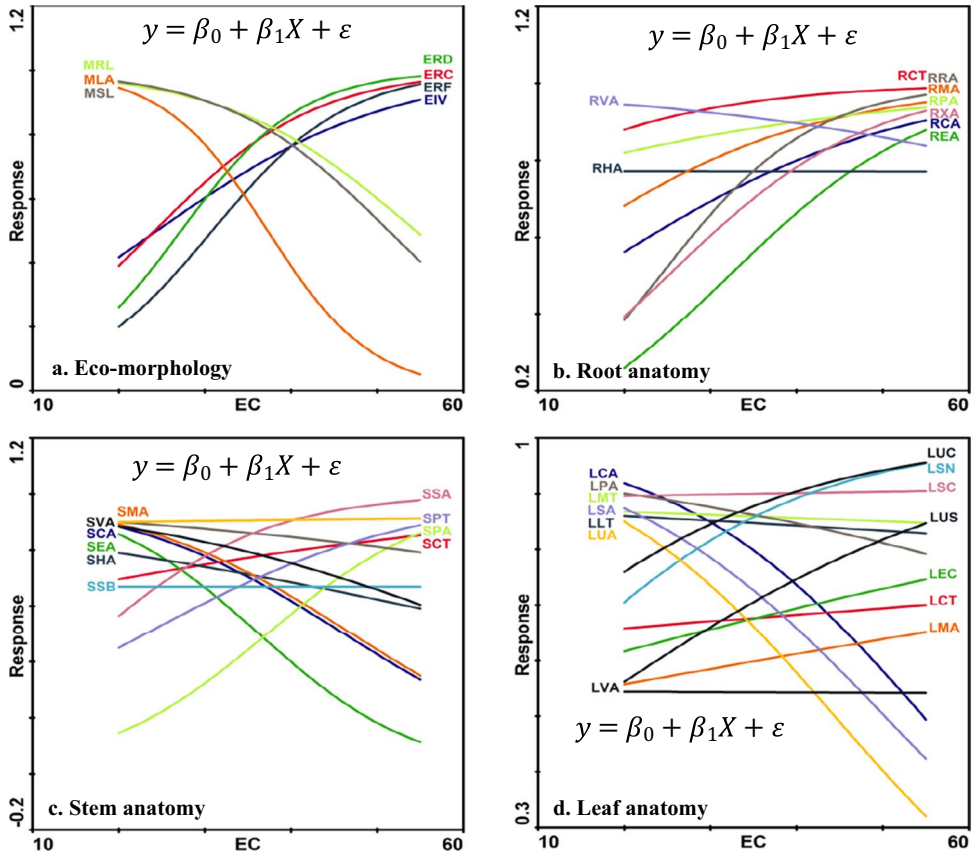


**Fig. 6** Generalized linear model (GLM) showing response curve for eco-morphological and anatomical traits of *Fagonia indica* collected from the Cholistan Desert. **a** Eco-morphology. **b** Root anatomy. **c** Stem anatomy. **d** Leaf anatomy. *Ecology*: ERF, relative density; ERD, relative frequency; EIV, importance value; ERC, relative cover. *Morphology*: MLA, total leaf area; MRL, root length; MSL, shoot length. Root anatomy: RRA, root cross-sectional area; RXA, exodermal cell area; RHA, hypodermal cell area; RCT, cortical thickness; RCA, cortical cell area; REA, endodermal cell area; RPA, pericycle cell area; RMA, metaxylem area; RVA, phloem area. *Stem anatomy*: SSA, stem cross-sectional area; SEA, epidermal cell area; SHA, hypodermal cell area; SCT, cortical thickness; SCA, cortical cell area; SMA, metaxylem area; SVA, phloem area; SPT, pith thickness; SPA, pith cell area; SSB, sclerenchyma bundle area. *Leaf anatomy*: LSN, abaxial stomatal density; LUS, adaxial stomatal density; LSA, abaxial stomatal area; LUA, adaxial stomatal area; LMT, midrib thickness; LLT, lamina thickness; LEC, abaxial epidermal cell area; LUC, adaxial epidermal cell area; LCT, adaxial epidermal cell area; LCA, parenchymatous cell area; LPA, palisade cell area; LSC, spongy cell area; LMA, metaxylem area; LVA, phloem area

Phytoremediation parameters like shoot and root Cl − dilution factor responded strongly positively along increasing salinity gradient, whereas $Na^+$ translocation factor showed a negative slope. Root and shoot $Na^+$ dilution factor and $Cl^-$ translocation factor showed a linear response (Fig. 7 c).

## Discussion

The populations of *F. indica* were collected from different areas of extremely hot, arid, and saline conditions of the Cholistan Desert. The populations inhabiting variously salt-affected areas attained differential structural and functional modifications (Fig. 8), which may have contributed to their sustainability under saline conditions, phytoremediation of salt-affected soils, and for rehabilitation of saline lands (Kaleem and Hameed 2021a). Desalination with halophytes with high adaptability, salinity tolerance, and growth potential is the only solution for the removal of $Na^+$ under non-leaching conditions. Halophytes adopt different structural and functional approaches to tolerate high salinities. Ion accumulators (also referred as hyper-accumulators) store ions in aboveground plant parts. Examples are *Fimbristylis complanata* (Retz.) Link (Kaleem and Hameed 2021a), *Suaeda vera* Forssk. ex J. F. Gmel. (Asghar et al. 2022), and *Caroxylon imbricatum* (Forssk.) Moq. (Naz et al. 2021). The second group is of salt excrating species like *A. lagopoides* (Naz et al. 2018), *Sporobolus arabicus* Boiss. (Hameed et al. 2013), and *A. adscensionis* (Fatima et al. 2018).

Salinity causes ionic imbalance, induces oxidative stress, and perturbs essential metabolic processes in plants. Maintenance of ion homeostasis is one of the major fundamental

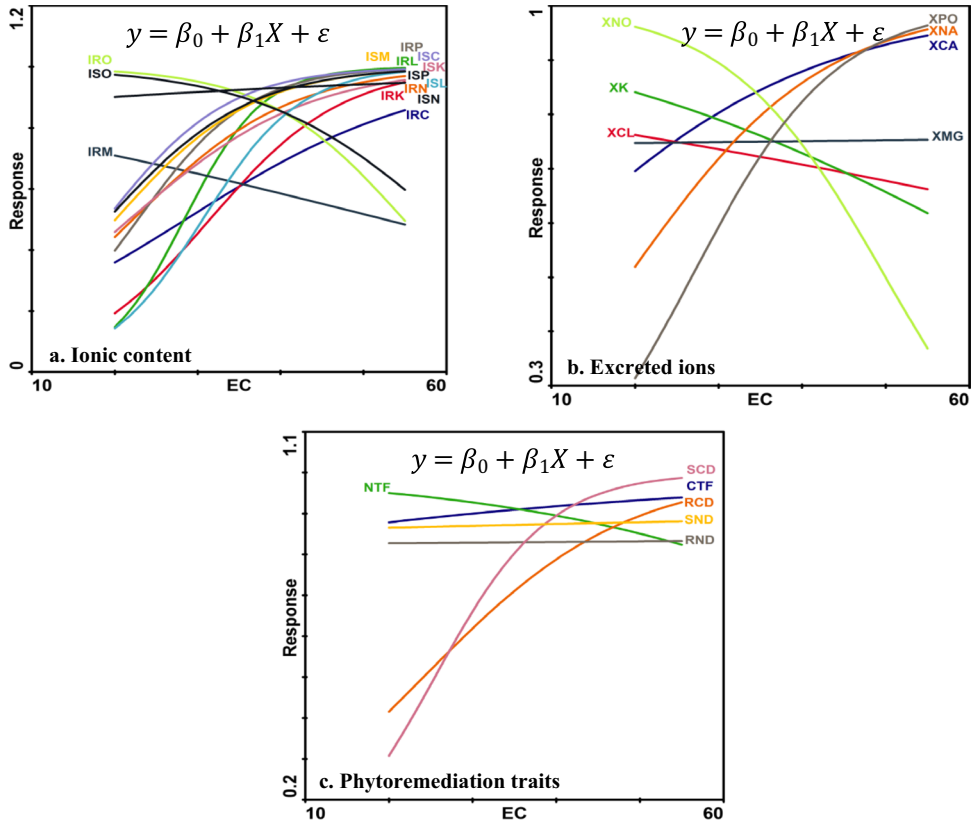


**Fig. 7** Generalized linear model (GLM) showing response curve for ionic content and excreted ions of *Fagonia indica* collected from the Cholistan Desert. **a** Ionic content. **b** Excreted ions. **c** Phytoremediation. *Ionic content*: ISN, shoot $Na^+$; IRN, root $Na^+$; ISK, shoot $K^+$; IRK, root $K^+$; ISC, shoot $Ca^{2+}$; IRC, root $Ca^{2+}$; ISL, shoot $Cl^-$; IRL, root $Cl^-$; ISM, shoot $Mg^{2+}$; IRM, root $Mg^{2+}$; ISP, shoot $PO_4^{3-}$; IRP, root $PO_4^{3-}$; ISO, shoot $NO_3^-$; IRO, root $NO_3^-$. *Excreted ions*: XNA, excreted $Na^+$; XK, excreted $K^+$; XCL, excreted $Cl^-$; XPO, excreted $PO_4^{3-}$; XNO, excreted $NO_3^-$; XMG, excreted $Mg^{2+}$; XCA, excreted $Ca^{2+}$. *Phytoremediation traits*: RNB, root $Na^+$ bioconcentration factor; RCB, root $Cl^-$ bioconcentration factor; RND, root $Na^+$ dilution factor; RCD, root $Cl^-$ dilution factor; SNB, shoot $Na^+$ bioconcentration factor; SCB, shoot $Cl^-$ bioconcentration factor; SND, $Na^+$ dilution factor; SCD, shoot $Cl^-$ dilution factor; NTF, $Na^+$ translocation factor; CTF, $Cl^-$ translocation factor; IEE, ion excretion efficiency

processes in salt-tolerant plants mediated through various adaptive strategies (Chakraborty et al. 2018). Plants accomplish various ion homeostasis mechanisms like salt exclusion, increased succulence, vacuolar compartmentalization, and compatible solute accumulation. Kaleem et al. (2022) reported similar findings in *F. complanata*. High concentrations of root and shoot $Na^+$ in the highly saline population Pati Sir reduced substantially. Restricted uptake of $Na^+$ in root and shoots is considered as a preventive strategy of the plant to overcome cytosolic ionic toxicity (Muchate et al. 2016). Shoot $K^+$ markedly increased in the highly saline population Pati Sir, while the Ladam Sir population exhibited substantial amounts of $K^+$ in roots. Such accumulation of $K^+$ during salinity stress plays a key role in osmotic adjustments and could drive cell singling during salinity stress (Wu et al. 2018). Mohammadi et al. (2019) reported similar findings in *Leptochloa fusca* (L.) Kunth. These high levels of $K^+$ also initiate "metabolic switch" to inhibit energy-dependent biochemical processes to conserve energy at the cellular level (Demidchik et al. 2014). The $Ca^{2+}$ exhibited more accumulation in response to higher salinities at the root and shoot levels in *F. indica*, as an increase in extracellular salt regimes has been reported to rapidly increase cytosolic $Ca^{2+}$ concentrations (Isayenkov and Maathuis 2019). The corresponding influx of $Ca^{2+}$ is actively involved in ROS signaling and increase salt tolerance in plants, as was reported by Joshi et al. (2022). The concentration of $Cl^-$ ion increased in the root and shoot in *F. indica*. Salinity-induced dilemma increases the level of $Cl^-$, which provides a cheap osmoticum in roots and shoots to lower the osmotic potential (Isayenkov and Maathuis 2019). The level of $Mg^{2+}$ at the root and shoot levels was also elevated along salinity gradients, as it is a vital divalent cation for effective metabolic and physiological functioning of plants, especially under stress environments, which can maintain the cytosolic pH and $Ca^{2+}$ ion homeostasis as well as carbohydrate allocation from root to shoot (Koksal et al. 2016).

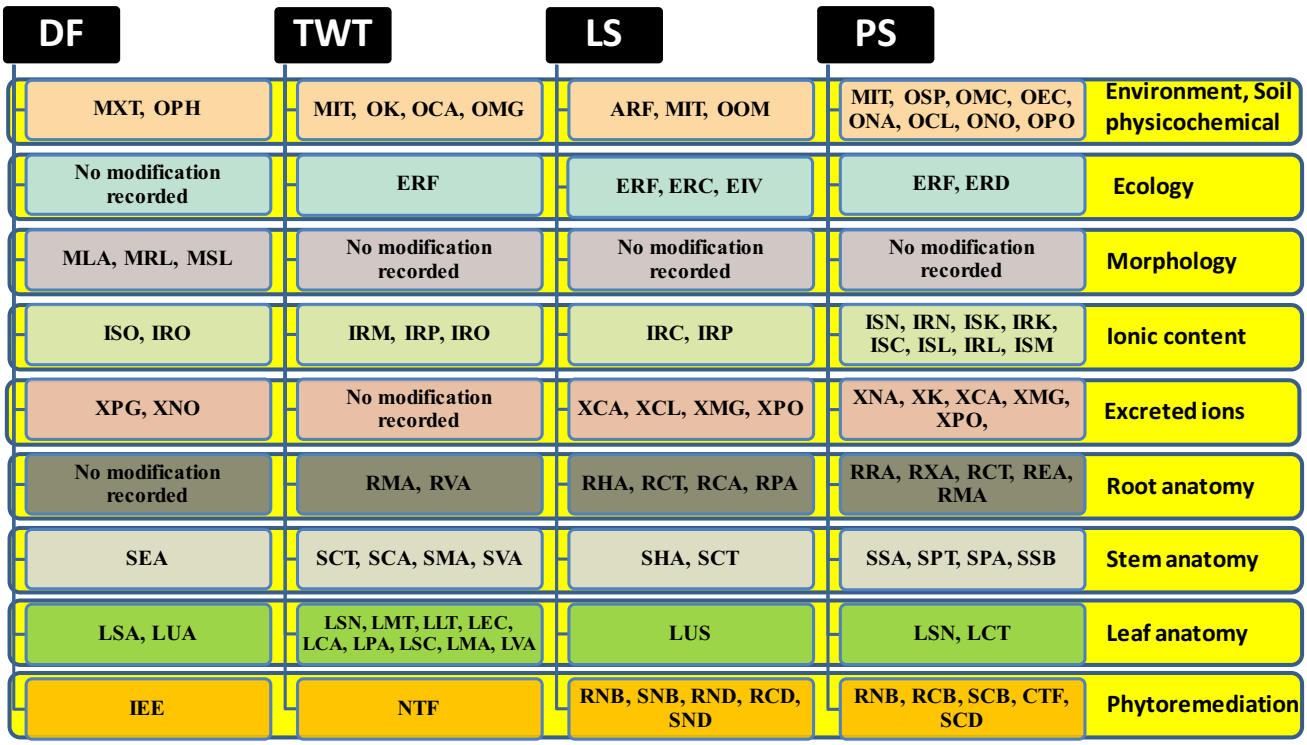


**Fig. 8** Flowchart showing overall structural, functional, and phytoremediation response of *Fagonia indica* populations from the Cholistan Desert. Collection site: DF, Derawar Fort; TWT, Traway Wala Toba; LS, Ladam Sir; PS, Pati Sir. *Weather*: ARF, annual rainfall; MIT, minimum mean temperature; MXT, maximum mean temperature. *Soil properties*: OPH, soil pH; OEC, soil ECe; ONA, soil $Na^+$; OK, soil $K^+$; OCA, soil $Ca^{2+}$; OMG, soil $Mg^{2+}$; OCL, soil $Cl^-$; ONO, soil $NO_3^-$; OPO, soil $PO_4^{3-}$; OSP, saturation percentage; OMC, moisture content; OOM, organic matter. *Ecology*: ERF, relative density; ERD, relative frequency; EIV, importance value; ERC, relative cover. Morphology: MLA, total leaf area; MRL, root length; MSL, shoot length. Root anatomy: RRA, root cross-sectional area; RXA, exodermal cell area; RHA, hypodermal cell area; RCT, cortical thickness; RCA, cortical cell area; REA, endodermal cell area; RPA, pericycle cell area; RMA, metaxylem area; RVA, phloem area. *Stem anatomy*: SSA, stem cross-sectional area; SEA, epidermal cell area; SHA, hypodermal cell area; SCT, cortical thickness; SCA, cortical cell area; SMA, metaxylem area; SVA, phloem area; SPT, pith thickness; SPA, pith cell area; SSB, sclerenchyma bundle area. *Leaf anatomy*: LSN, abaxial stomatal density; LUS, adaxial stomatal density; LSA, abaxial stomatal area; LUA, adaxial stomatal area; LMT, midrib thickness; LLT, lamina thickness; LEC, abaxial epidermal cell area; LUC, adaxial epidermal cell area; LCT, adaxial epidermal cell area; LCA, parenchymatous cell area; LPA, palisade cell area; LSC, spongy cell area; LMA, metaxylem area; LVA, phloem area. *Ionic content*: ISN, shoot $Na^+$; IRN, root $Na^+$; ISK, shoot $K^+$; IRK, root $K^+$; ISC, shoot $Ca^{2+}$; IRC, root $Ca^{2+}$; ISL, shoot $Cl^-$; IRL, root $Cl^-$; ISM, shoot $Mg^{2+}$; IRM, root $Mg^{2+}$; ISP, shoot $PO_4^{3-}$; IRP, root $PO_4^{3-}$; ISO, shoot $NO_3^-$; IRO, root $NO_3^-$. *Excreted ions*: XNA, excreted $Na^+$; XK, excreted $K^+$; XCL, excreted $Cl^-$; XPO, excreted $PO_4^{3-}$; XNO, excreted $NO_3^-$; XMG, excreted $Mg^{2+}$; XCA, excreted $Ca^{2+}$. *Phytoremediation traits*: RNB, root $Na^+$ bioconcentration factor; RCB, root $Cl^-$ bioconcentration factor; RND, root $Na^+$ dilution factor; RCD, root $Cl^-$ dilution factor; SNB, shoot $Na^+$ bioconcentration factor; SCB, shoot $Cl^-$ bioconcentration factor; SND, $Na^+$ dilution factor; SCD, $Cl^-$ dilution factor; NTF, $Na^+$ translocation factor; CTF, $Cl^-$ translocation factor; IEE, ion excretion efficiency

The distribution and ecology of *F. indica* were not much affected due to increasing levels of salinity stress, which indicated their tolerance potential to specific habitats containing varying levels of salinity. The relative frequency of the Pati Sir population of *F. indica* was higher under extreme hot and hypersaline conditions with 51 dS $m^{-1}$ ECe level and 5312 mg $L^{-1}$ soil Na, indicating a wider distribution in these habitats due to better adaptive strategies. However, relative density, cover, and importance value were higher in Ladam Sir population with second highest soil ECe (39 dS $m^{-1}$) and Na (4556 mg $L^{-1}$). Similar results were reported by Naz et al. (2015) in *L. scindicus* and Fatima et al. (2021) in *C. jwarancusa* (Jones) Schult. collected from the Cholistan Desert. Growth performance either of root or shoot under saline conditions is a good criterion to check the tolerance potential in plants (El-Hendawy et al. 2017). Root and shoot growth is generally sensitive to salinity stress, but there is a considerable variation among species or ecotypes of a single species. Leaf area and biomass production generally decrease along the increasing salinity gradients, as was recorded in the present study, indicating cell growth cessation as an immediate response of salt stress (Kotagiri and Kolluru 2017). Generally, populations from highest salinities (Ladam Sir, 39 dS $m^{-1}$; PS, 51 dS $m^{-1}$) showed restricted

vegetative growth but were tolerant to the effects of high salinities in their respective habitats, indicating their potential to remediate hypersaline soils.

Salinity stress led to specific anatomical changes in *F. indica*. Numbers of abaxial and adaxial epidermal cells increased as salinity levels increased. It has been reported that salt-tolerant plants possess thickened epidermis to minimize water loss in arid climates (Kaleem and Hameed 2021b; Terletskaya et al. 2022). The numbers of stomata increased particularly at abaxial than adaxial epidermis because of higher salinities. Such change in stomatal number is directly linked to salinity tolerance for better survival by controlling transpiration (Cavusoglu et al. 2008). Leaf epidermal cells decreased on both leaf surfaces in populations from hypersaline habitats that might be attributed to the growth and cell division limitations imposed by salinity stress (Parida et al. 2016). Leaf succulence (midrib and lamina thickness) increased in the Traway Wala Toba population. This increase might be a counter effect of enhanced $Na^+$ exclusion from the cytosol to the leaf tissues. Enhanced succulence phenomenon also increases vacuolar size to sequester $Na^+$ away from the metabolic hub of the cell (Shabala 2013).

Epidermal thickness and cell area exhibited a variable response in all populations, and abaxial and adaxial epidermal thickness increased in the Pati Sir and Ladam Sir populations, respectively. Thickened epidermis is considered as an important check to ensure water conservation, a vital commodity during salt-induced physiological drought. Higher salinities caused a reduction in parenchymatous cell area, which ultimately led to curtail the reduced leaf surface area. Palisade and spongy thickness and area were significantly reduced in the highly saline Pati Sir population. This reduction might be an energy-saving process to reduce gaseous exchange in the spongy mesophyll cells (Akcin et al. 2017). Leaf phloem area increased in the Traway Wala Toba population to facilitate better conduction of photosynthetic products from source to sink.

Root cross-sectional area in the Ladam Sir population collected from highly saline conditions, mainly due to proportion of parenchymatous or stelar region (Hameed et al. 2011), such modification improves storage and conduction of water and nutrients. Root exodermal and hypodermal cell area and thickness also increased with increasing salt levels. This is a critical adaptation as thickened exodermis prevents the excess water loss during salinity stress (Hameed et al. 2013). Cortex thickness and cell area increased in the Pati Sir and Ladam Sir population, respectively. An increase in root area effectively impedes salinity-induced osmotic stress by enhancing the storage capacity of plants (Naz et al. 2016). Endodermal and pericycle thickness and area increased markedly with an increase in salinity of the habitat. Thickened pericycle and endodermis reduce water loss from the stelar region (Ahmad et al. 2016). Higher salinities did not alter the metaxylem area of root in the Traway Wala Toba and PS populations. Those salt-tolerant plants equipped with larger metaxylem vessels are believed to be vibrant for enhanced conduction of water. The phloem area decreased at high salinities, so reduction in this trait is due to stunted growth (Naz et al. 2015).

At stem level, stem cross-sectional area increased in the Pati Sir population inhabiting the highly saline area. Change in cross-sectional area in desert species is more advantageous because it resists abiotic stresses. An increase in stem cross-sectional area along with storage parenchyma (cortex and pith) enhances water storage capacity of the stem (Corrêa et al. 2016). A significant reduction occurred in epidermal cell area along the salinity gradients in this study, indicating a preferable strategy to control water loss in arid environments (Naz et al. 2016). Hypodermal cell area and thickness markedly increased in the Ladam Sir and PS populations. These are critical modifications of desert plants to conserve maximum water when they are subjected to drought (or physiological drought) conditions over a longer period (Parida et al. 2016). Stem cortical thickness reduced, because higher salinities trigger deterioration of tissues (Eisa 2017). This is also beneficial to curtail plant growth and reduce energy expenditure. Stem anatomical traits like metaxylem and phloem area reduced in *F. indica* populations along salinity gradient. A decrease in conducting vessel diameter is usually involved in reduction of hydraulic activities and conferring safety to the conducing vessels (Junghans et al. 2006). Reduction in xylem and phloem diameters ultimately reduces the translocation of nutrients to the aerial parts or back to the underground organs, which confer changes in growth under higher salinities. Pith area and thickness generally increase in plants growing at higher salinities that improve succulence and critically important for desert inhabitants (Parida et al. 2016). Sclerenchyma bundle and cell area increased with an increase in salinity in all *F. indica* populations. The development of sclerenchyma provides a mechanical strength during salt stress and osmotic stress (Alvarez et al. 2008).

The moderately saline population Traway Wala Toba had a high proportion of palisade and spongy mesophyll cell area in leaves, while higher salinities resulted in reduction of these traits. Palisade and spongy mesophylls directly anticipate photosynthesis due to large number of chloroplasts (Paradiso et al. 2017). Toxic $Na^+$ and $Cl^-$ accumulated primarily in vacuoles of photosynthetically active mesophyll cells; therefore, any change in palisade parenchyma caused by extreme salinities directly influences phytoremediation capacity of *F. indica*. Such reduction as observed at high salinities can either be regarded as a direct influence of salinity stress or an adaptive response to decrease expenditures of photosynthetic energy utilization (Parida et al. 2016).

The moderately saline population Traway Wala Toba had wider metaxylem and phloem vessels in leaves as compared to those in its corresponding populations. These conduits help in better conduction of water, nutrients, and photoassimilates. The increased vascular tissue area with elevated salinity gradients guaranteed better conduction of nutrients without any obstruction (Shabala and Munns 2012).

The utilization of halophytes is a cheap and effective strategy for reclamation of salt-affected soils. Many researches previously used halophytes for the phytoremediation of saline soils, for example, *S. maritima* and *S. portulacastrum* (Ravindran et al. 2007), *S. europaea*, *S. soda*, and *T. qatarensis* (Yasseen and Al-Thani 2022). Halophytes generally accumulate $Na^+$ in cytosol in high concentrations. Size of the parenchymatous cells (cortical and pith parenchyma and mesophyll tissue) is associated with large-sized vacuoles, i.e., having more capacity to store $Na^+$ and $Cl^-$ (Franceschi and Loewus 2020). Size of parenchymatous cells increased in *F. indica* population along salinity levels in most organs. Salt exclusion is the other mechanism related to phytoremediation. Consistently increased density salt glands and excreted $Na^+$ is an indication of potential phytoremediation capacity of *F. indica*.

The prominent findings are increased density, frequency, and importance value along salinity gradient is an indication of high salinity tolerance of *F. indica* in the Cholistan Desert. Morphological features like plant height, root length, and total leaf area decreased significantly with salinity level, which not only will reduce transpiration rate but may spent more energy towards survival rather than normal vegetative growth. The Pati Sir population from the highest salinity accumulated the maximum $Na^+$ and $Cl^-$ in root and shoot, the maximum shoot $Ca^{2+}$, and excreted maximum concentration of $Na^+$ from the leaves. Root traits such as increased thicknesses of exodermis and endodermis prevent radial flow of water from roots, hence critical for water conservation. Increased metaxylem area is directly related to better water and nutrient conduction. Stem traits such as increased stem cross-sectional area, which is primarily due to pith tissue, and increased sclerification can be linked to water conservation by preventing water loss and storing more water inside stem tissues.

Leaf features such as decreased stomatal area on adaxial (upper) leaf surface in a critical modification in the Pati Sir population. The upper leaf surface is more exposed to external environments, and smaller stomata on adaxial surface can limit transpiration rate, which is critical for the survival in hot, saline, and hyper-arid conditions. Moreover, a significant increase in adaxial epidermis can prevent water loss from leaf surface, which is a characteristic of desert plants. Density of salt glands remarkably increased in the Pati Sir population, which is the justification of high excretion rate of $Na^+$. In our study, bioconcentration factor, translocation factor, and dilution factor of $Cl^-$ were the maximum at the highest saline Pati Sir sites while that of $Na^+$ at the highly saline Ladam Sir sites. The plants of *F. indica* colonizing high salinities were, therefore, more efficient in phytoremediation of saline soils.

Among limitations, we collected *F. indica* from natural habitats, the modification might be due to a specific set of environmental conditions. To investigate genetically fixed traits, this species has to evaluate in a controlled greenhouse conditions, so that these traits can express themselves.

## Conclusion

During a long-term evolutional process, each population of *F. indica* acquired some specific adaptive components which enabled thriving under the specific environmental attributes of native habitats. As was hypothesized, several root, stem, and leaf anatomical traits were found linked to phytoremediation potential of *F. indica*. These included increased cross-sectional areas of root and stem; high proportion of storage parenchyma; increased thicknesses of epidermis, exodermis, and endodermis; broad metaxylem vessels; better compartmentalization and excretion of toxic $Na^+$ and $Cl^-$; and size and density of its salt-excretory glands. More importantly, the dilution factor was the highest in the Pati Sir population. Variation in phytoremediation-related structural and functional features (research question a) was exceptionally high among the populations of *F. indica*, which can be used to identify the most suitable populations of *F. indica* and other associated species (research question b) for phytoremediation of saline soils.

**Supplementary Information** The online version contains supplementary material available at https://doi.org/10.1007/s11356-023-28162-z.

**Acknowledgements** This manuscript is derived partly from the PhD thesis of the first author submitted to Botany Department, University of Agriculture Faisalabad, Pakistan.

**Author contribution** Nargis Naz, principal author conducted the experiment and compiled the manuscript. Mansoor Hameed, supervisor and planned the research project. Farooq Ahmad and Muhammad Ashraf, members of the student's advisory committee and helped in research planning, sample collection, and execution of research. Muhammad Sajid Aqeel Ahmad, statistical experts, data compilation, visualization, modeling, and interpretation. Syed Mohsan Raza Shah, Sana Fatima, Majid Anwar, Sana Basharat, and Ansa Asghar, members of the research team, sample collection, analytical analysis, and manuscript writing.

**Data availability** The herbarium samples of plant collections along with voucher numbers are deposited in the Herbarium Collection of the Department of Botany, University of Agriculture Faisalabad. The primary data generated in this study along with original micrographs captured through digital microscope are available with the second

author and can be requested if needed to reproduce data visualizations and modeling.

## Declarations

**Ethical approval** The study does not include any animal or human subjects, and no specific ethical approval is needed. Other necessary guidelines set by University of Agriculture, Faisalabad, for handling of plant material during conduction of laboratory work were followed. All samplings were done with the least possible disturbances to plant communities and environment. After completion of study, all experimental materials were properly discarded/incinerated in a controlled environment to avoid bio-contamination.

**Consent to participate** The contribution of all participants/parties involved in this study has been appreciated either in authorship OR acknowledged in the acknowledgement section. All contributors listed in this manuscript have substantially participated in this study and preparation of the manuscript.

**Consent for publication** It is certified that the manuscript is the product of an original study and is submitted solely to this journal for consideration. It is not submitted to any other journal, in part or full, for simultaneous consideration nor has been previously published in any form or language (other than as a thesis of the first author, which is properly acknowledged). There is no plagiarism/self-plagiarism, salami-slicing/publishing, secondary publication nor near verbatim. All data presented in this manuscript is the product of our own study, and the manuscript does not contain any copyrighted material (data tables or figures). All results and data are presented clearly, honestly, and without fabrication, falsification, or inappropriate data manipulation (including image-based manipulation). All authors agree to publish, and there is no conflict for publication of this manuscript for publication in this journal.

**Conflict of interest** The authors declare no competing interests.

## References


Ahmad M, Eram S (2011) Hepatoprotective studies on *Haloxylon salicornicum*: a plant from Cholistan Desert. Pak J Pharmacol Sci 24:377–382

Ahmad KS, Hameed M, Deng J, Ashraf M, Hamid A, Ahmad F, Fatima S, Akhtar N (2016) Ecotypic adaptations in Bermuda grass (*Cynodon dactylon*) for altitudinal stress tolerance. Biologia 71:885–895

Ahmed N, Mahmood A, Tahir SS, Bano A, Malik RN, Hassan S, Ashraf A (2014) Ethnomedicinal knowledge and relative importance of indigenous medicinal plants of Cholistan Desert, Punjab province, Pakistan. J Ethnopharmacol 155:1263–1275

Akcin TA, Akcin A, Yalcın E (2017) Anatomical changes induced by salinity stress in *Salicornia freitagii* (Amaranthaceae). Braz J Bot 40:013–1018

Al-Nasir F (2009) Bioreclamation of a saline sodic soil in a semi arid region/Jordan. Am-Eur J Agric Environ Sci 5:701–706

Alsihany MM, Ghoneim AM, Bukhari NA (2019) Transfer and accumulation of some heavy metals in native vegetation plants. Int J Plant Soil Sci 28:1–10

Alvarez JM, Rocha JF, Machado SR (2008) Bulliform cells in *Loudetiopsis chrysothrix* (Nees) Conert and *Tristachya leiostachya* Nees (Poaceae): structure in relation to function. Braz Arch Biol Technol 51:113–119

Asghar N, Hameed M, Ahmad MSA (2022) Ion homeostasis in differently adapted populations of Suaeda vera Forssk. ex. J.F. Gmel. for phytoremediation of hypersaline soils. Int J Phytorem. https://doi.org/10.1080/15226514.2022.2056134

Bose J, Munns R, Shabala S, Gilliham M, Pogson B, Tyerman SD (2017) Chloroplast function and ion regulation in plants growing on saline soils: lessons from halophytes. J Exp Bot 68:3129–3143

Castro FC, Santos AMD (2020) Salinity of the soil and the risk of desertification in the semiarid region. Mercator (fortaleza) 9:19

Cavusoglu K, Kilic S, Kabar K (2008) Effects of some plant growth regulators on stem anatomy of radish seedlings grown under saline (NaCl) conditions. Plant Soil Environ 54:428–433

Chakraborty K, Basak N, Bhaduri D, Ray S, Vijayan J, Chattopadhyay K, Sarkar RK (2018) Ionic basis of salt tolerance in plants: nutrient homeostasis and oxidative stress tolerance. In: Hasanuzzaman M, Fujita M, Oku H, Nahar K, Hawrylak-Nowak B (eds) Plant nutrients and abiotic stress tolerance. Springer, Singapore, pp 325–362

Corrêa FF, Pereira MP, Madail RH, Santos BR, Barbosa S, Castro EM, Pereira FJ (2016) Anatomical traits related to stress in high density populations of *Typha angustifolia* L. (Typhaceae). Braz J Biol 77:52–59

Demidchik V, Straltsova D, Medvedev SS, Pozhvanov GA, Sokolik A, Yurin V (2014) Stress-induced electrolyte leakage: the role of K+-permeable channels and involvement in programmed cell death and metabolic adjustment. J Exp Bot 65:1259–1270

Diwan H, Ahmad A, Iqbal M (2010) Uptake-related parameters as indices of phytoremediation potential. Biologia 65:1004–1011

Eisa GSA (2017) Drought and salt stress induced anatomical changes in leaves and stems of Indian borage plants (*Plectranthus amboinicus*, (Loureiro) Sprengel). Menoufia J Plant Prod 2:25–37

El-Hendawy SE, Hassan WM, Al-Suhaibani NA, Refay Y, Abdella KA (2017) Comparative performance of multivariable agro-physiological parameters for detecting salt tolerance of wheat cultivars under simulated saline field growing conditions. Front Plant Sci 8:435

Fatima S, Ahmad F, Hameed M, Ahmad R (2018) Ecology and species association of grass species in response to altitudinal gradient in the Potohar region. Pak J Bot 50:41–49

Fatima S, Hameed M, Naz N, Shah SMR, Naseer M, Ahmad MSA, Ashraf M, Ahmad F, Khalil S, Ahmad I (2021) Survival strategies in Khavi grass [*Cymbopogon jwarancusa* (Jones) Schult.] colonizing hot hypersaline and arid environments. Water Air Soil Pollut 232:1–17

Franceschi VR, Loewus FA (2020) Oxalate biosynthesis and function in plants and fungi. In: Khan SR (ed) Calcium Oxalate in Biological Systems. CRC press, Wales, UK, pp 113−130

Gavrilescu M (2022) Enhancing phytoremediation of soils polluted with heavy metals. Curr Opin Biotechnol 74:21–31

Ghoneim AM, Al-Zahrani S, El-Maghraby S, Al-Farraj AS (2014) Heavy metals accumulation in *Rhazya stricta* L. plant growing on industrial wastewater of Riyadh city, Saudi Arabia. J Appl Sci 14:2007–2010

Hameed M, Ashraf M, Naz N (2011) Anatomical and physiological characteristics relating to ionic relations in some salt tolerant grasses from the Salt Range, Pakistan. Acta Physiol Plant 33:1399–1409

Hameed M, Ashraf M, Naz N, Nawaz T, Batool R, Ahmad MSA, Ahmad F, Hussain M (2013) Anatomical adaptations of *Cynodon dactylon* (L.) Pers. from the Salt Range (Pakistan) to salinity stress. II. Leaf anatomy. Pak J Bot 45:133–142

Isayenkov SV, Maathuis FJ (2019) Plant salinity stress: many unanswered questions remain. Front Plant Sci 10:80

Joshi S, Nath J, Singh AK, Pareek A, Joshi R (2022) Ion transporters and their regulatory signal transduction mechanisms for salinity tolerance in plants. Physiol Plant 174:e13702

Junghans U, Polle A, Düchting P, Weiler E, Kuhlman B, Gruber F, Teichmann T (2006) Adaptation to high salinity in poplar involves changes in xylem anatomy and auxin physiology. Plant Cell Environ 29:1519–1531

Kaleem M, Hameed M (2021a) Functional traits for salinity tolerance in differently adapted populations of *Fimbristylis complanata* (Retz.). Inter J Phytorem 23:1319–1332

Kaleem M, Hameed M (2021b) Plasticity in structural and functional traits associated with photosynthesis in *Fimbristylis complanata* (Retz.) Link. under salt stress. Int J Phytorem 53:1199–1208. https://doi.org/10.30848/PJB2021-4(28)

Kaleem M, Hameed M, Ahmad F, Ashraf M, Ahmad MSA (2022) Anatomical and physiological features modulate ion homeostasis and osmoregulation in aquatic halophyte Fimbristylis complanata (Retz.) Link. Acta Physiol Plant 44:59

Kanwal N, Adhikari A, Hameed A, Musharraf HRM, SG, (2017) Isolation and characterization of non-sulfated and sulfated triterpenoid saponins from *Fagonia indica*. Phytochemistry 143:151–159

Khan MA, Qaiser M (2006) Halophytes of Pakistan: characteristics, distribution and potential economic usages. In: Khan MA, Böer B, Kust GS, Barth HJ (eds) Sabkha Ecosystems. Tasks for Vegetation Science, vol 42. Springer, Dordrecht. https://doi.org/10.1007/978-1-4020-5072-5_11

Khan MA, Weber DJ (2006) Soil remediation via salt-conduction and the hypotheses of halosynthesis and photoprotection. In: Khan MA, Weber DJ (eds) Ecophysiology of High Salinity Tolerant Plants. Tasks for Vegetation Science, vol 40. Springer, NY

Koksal N, Alkan-Torun A, Kulahlioglu I, Ertargin E, Karalar E (2016) Ion uptake of marigold under saline growth conditions. Springerplus 5:1–12

Kotagiri D, Kolluru VC (2017) Effect of salinity stress on the morphology and physiology of five different *Coleus* species. Biomed Pharmacol J 10:1639–1649

Kowalenko CG, Lowe LE (1973) Determination of nitrates in soil extracts. Soil Sci Soc Am J 37:660

Mansoor U, Fatima S, Hameed M, Naseer M, Ahmad MSA, Ashraf M, Ahmad F, Waseem M (2019) Structural modifications for drought tolerance in stem and leaves of Cenchrus ciliaris L. ecotypes from the Cholistan Desert. Flora 261:151485

Mohammadi F, Kavousi HR, Mansouri M (2019) Effects of salt stress on physio-biochemical characters and gene expressions in halophyte grass *Leptochloa fusca* (L.) Kunth. Acta Physiol Plant 41:1–10

Muchate NS, Nikalje GC, Rajurkar NS, Suprasanna P, Nikam TD (2016) Plant salt stress: adaptive responses, tolerance mechanism and bioengineering for salt tolerance. Bot Rev 82:371–406

Naz N, Batool R, Fatima S, Hameed M, Ashraf M, Ahmad F, Ahmad MSA (2015) Adaptive components of tolerance to salinity in a saline desert grass *Lasiurus scindicus* Henrard. Ecol Res 30:429–438

Naz N, Fatima S, Hameed M, Naseer M, Batool R, Ashraf M, Ahmad F, Ahmad MSA, Zahoor A, Ahmad KS (2016) Adaptations for salinity tolerance in *Sporobolus ioclados* (Nees ex Trin.) Nees from saline desert. Flora 223:46–55

Naz N, Fatima S, Hameed M, Ashraf M, Naseer M, Ahmad F, Zahoor A (2018) Structural and functional aspects of salt tolerance in differently adapted ecotypes of *Aeluropus lagopoides* from saline desert habitats. Int J Agric Biol 20:41–51

Naz N, Fatima S, Hameed M, Ahmad F, Ahmad MSA, Ashraf M, Shahid H, Iqbal U, Kaleem M, Shah SMR, Ahmad I (2021) Modulation in plant micro-structures through soil physicochemical properties determines survival of *Salsola imbricata* Forssk. in hypersaline environments. J Soil Sci Plant Nutr 22:861–881

Paradiso R, Arena C, De Micco V, Giordano M, Aronne G, De Pascale S (2017) Changes in leaf anatomical traits enhanced photosynthetic activity of soybean grown in hydroponics with plant growth-promoting microorganisms. Front Plant Sci 8:674

Parida AK, Veerabathini SK, Kumari A, Agarwal PK (2016) Physiological, anatomical and metabolic implications of salt tolerance in the halophyte Salvadora persica under hydroponic culture condition. Front Plant Sci 7:351

Ravindran KC, Venkatesan K, Balakrishnan V, Chellappan KP, Balasubramanian T (2007) Restoration of saline land by halophytes for Indian soils. Soil Biol Biochem 39:2661–2664

Richards LA (1954) Diagnosis and improvement of. saline and alkali soils. United States Salinity Laboratory Staff Agricultural Handbook No. 60, p. 160, United States Department of Agriculture, US Government Printing Office, Washington, DC

Ruzin SE (1999) Plant microtechnique and microscopy (Vol. 198, p. 322). New York: Oxford University Press

Satpute R, Bhattacharya R, Kashyap RS, Purohit HJ, Deopujari JY, Taori GM, Daginawala HF (2012) Antioxidant potential of *Fagonia arabica* against the chemical ischemia-induced in PC12 cells. Iran J Pharmaceut Res 11:303

Schrader J, Shi P, Royer DL, Peppe DJ, Gallagher RV, Li Y, Wang R, Wright IJ (2021) Leaf size estimation based on leaf length, width and shape. Ann Bot 128:395–406

Shabala S (2013) Learning from halophytes: physiological basis and strategies to improve abiotic stress tolerance in crops. Ann Bot 112:1209–1221

Shabala S, Munns R (2012) Salinity stress: physiological constraints and adaptive mechanisms. Plant Stress Physiol 1:59–93

Sims JR, Haby VA (1971) Simplified colorimetric determination of soil organic matter. Soil Sci 112:137–141

Terletskaya NV, Erbay M, Zorbekova AN, Prokofieva MY, Saidova LT, Mamirova A (2022) Influence of osmotic, salt, and combined stress on morphophysiological parameters of *Chenopodium quinoa* photosynthetic organs. Agriculture 13:1

Wolf B (1982) A comprehensive system of leaf analyses and its use for diagnosing crop nutrient status. Commun Soil Sci Plant Anal 13:1035–1059

Wu H, Zhang X, Giraldo JP, Shabala S (2018) It is not all about sodium: revealing tissue specificity and signalling roles of potassium in plant responses to salt stress. Plant Soil 431:1–17

Yasseen BT, Al-Thani RF (2022) Endophytes and halophytes to remediate industrial wastewater and saline soils: perspectives from Qatar. Plants 11:1497

Yoshida S, Forno DA, Cock JH (1971) Laboratory manual for physiological studies of rice. Laboratory manual for physiological studies of rice. The International Rice Research Institute Philippines, Los Baños, Philippines